Trabajo Fin de Máster
Máster en Ingeniería Industrial - Intensificación Energética

Analysis of supercritical carbon dioxide Brayton cycles for a DEMO-like fusion power plant

Autor: Javier Hidalgo Salaverri

Tutor: Ricardo Chacartegui Ramírez

Tutor: Juan Manuel Ayllón Guerola

Dpto. Máquinas y Motores Térmicos
Escuela Técnica Superior de Ingeniería
Universidad de Sevilla

Sevilla, 2020

Trabajo Fin de Máster

Máster en Ingeniería Industrial - Intensificación Energética

Analysis of supercritical carbon dioxide Brayton cycles for a DEMO-like fusion power plant

Autor:

Javier Hidalgo Salaverri

Tutor:

Ricardo Chacartegui Ramírez

Catedrático de Universidad

Tutor:

Juan Manuel Ayllón Guerola

Profesor Ayudante Doctor

Dpto. Máquinas y Motores Térmicos

Escuela Técnica Superior de Ingeniería

Universidad de Sevilla

Sevilla, 2020

Trabajo Fin de Máster: Analysis of supercritical carbon dioxide Brayton cycles for a DEMO-like fusion power plant

Autor: Javier Hidalgo Salaverri
Tutor: Ricardo Chacartegui Ramírez
Tutor: Juan Manuel Ayllón Guerola

El tribunal nombrado para juzgar el trabajo arriba indicado, compuesto por los siguientes profesores:

Presidente:

Vocal/es:

Secretario:

acuerdan otorgarle la calificación de:

El Secretario del Tribunal

Fecha:

Agradecimientos

A mi hermano y a mis padres, después de seis años de escuchar chorradas de ingeniero la dedicatoria de un TFM sabe a poco, pero al menos sé arreglar la impresora.

A mis tutores, por guiarme y animarme durante la realización de este trabajo y a lo largo de estos años.

Saber es noche

Abstract

Fusion energy is a clean, abundant and almost-unlimited power source for a future decarbonised energy market. The progressive disappearance of carbon-based power produced has sparked the necessity of finding reliable energy sources that can complement renewable energies. In this context, the international ITER project is aiming on demonstrating the physical and engineering feasibility of producing net thermal power from a nuclear fusion reactor. In parallel, the European Union is designing the next step after ITER, DEMO, a power plant whose goal is to be the first nuclear fusion power plant.

Currently, two designs are under research for DEMO: DEMO1, a conservative design based on a pulsed reactor and DEMO2, an optimistic approach where the reactor is working on steady-state. DEMO1 is the most established option as it is the most feasible one. DEMO1 is used as the current official design in the DEMO Baseline 2018. PROCESS is a system code developed by the Culham Centre for Fusion Energy (CCFE) that models fusion power plants from a physics and engineering point of view. This code has been used to obtain the DEMO Baseline 2018, that contains all the plasma physics and engineering parameters and constraints that define DEMO1.

A series of supercritical carbon dioxide (S-CO_2) Brayton cycles have been proposed for a DEMO-like fusion power plant. S-CO_2 Brayton cycles present good characteristics for fusion reactors as they present good efficiency for medium range temperatures (DEMO Baseline 2018 maximum temperature is 500ºC) and good tritium recovery (tritium is expected to leak into the carbon dioxide from the reactor). A total of eleven layouts are presented, nine for the pulsed DEMO1 and two for the steady-state DEMO2 scenario. As DEMO1 is a pulsed reactor, a thermal energy storage (TES) system is proposed to cover the gaps during pulses. For each layout, an optimization process has been carried out with the electric cycle efficiency as the figure of merit. For the pulsed state cases, a maximum efficiency of 34.47% is achieved and 56.1% for the steady-state.

The PROCESS code has been used to do an economic assessment of the most efficient pulsed layout and the two steady-state cases. This code estimates the plant cost and the cost of electricity (COE) of each layout. DEMO1 COE is set around 400$/MWh and 200$/MWh for DEMO2. This means that only the DEMO2 scenario is competitive with the current market prices. But subsidies are expected during the first generations of fusion

power plants as happened with renewable energies.

Contents

List of Figures

List of Tables

1 Introduction

Fusion energy is called to be an important part of the future electric mix. This work presents a set of layouts based on a supercritical carbon dioxide Brayton cycle for a fusion power plant. These layouts will be optimized and their total cost and the resulting cost of energy will be calculated using the PROCESS code. The objective of this chapter is to introduce the hypothetical role of fusion power in a future decarbonized economy. The physics and engineering basis needed for the core of this master's thesis is also introduced.

1.1 The energy situation

Climate change has unleashed a social uprising with a proportional response from governments from all over the world. Since the Kyoto Protocol in 2005, numerous international agreements have been signed by the biggest economical powers with the goal of reducing their climatic impact by, mainly, pouring less CO_2 into the atmosphere. This trend has increased as the public opinion started to voice more clearly its concern during the last decade. Due to this, more restrictive laws have been passed in Europe along other industrialized countries to cut their CO_2 emissions.

The decarbonization of the European economy has heavily impacted the power production industry, nowadays the market is under a total reconversion from a model based on carbon and natural gas to a new one with a significant percentage of renewable energies. The increasing fraction of renewable energies in the electric market has raised new issues that weren't important enough when they only represented a small slice of the cake. The two main renewable power producers, wind and solar energy, are strongly dependent on their sources and on the weather conditions and, in the case of solar power, not functioning for, at least, half of the day. This lack of availability and time flexibility requires nowadays of backup conventional power plants to ensure the normal supply of the grid. Energy storage has been envisioned as a possible solution, but current storage technologies are not up to the task.

With eyes on efficiency and zero pollution policies, the industrial fabric and European society is turning into a electrified society where some industrial processes and civil tasks

normally powered by fossil fuels, as transport or heating, are getting reconverted into an electrical equivalent. This means a higher electrical consumption that has to be covered by the electric grid and a more fluctuating production due to the presence of the renewables.

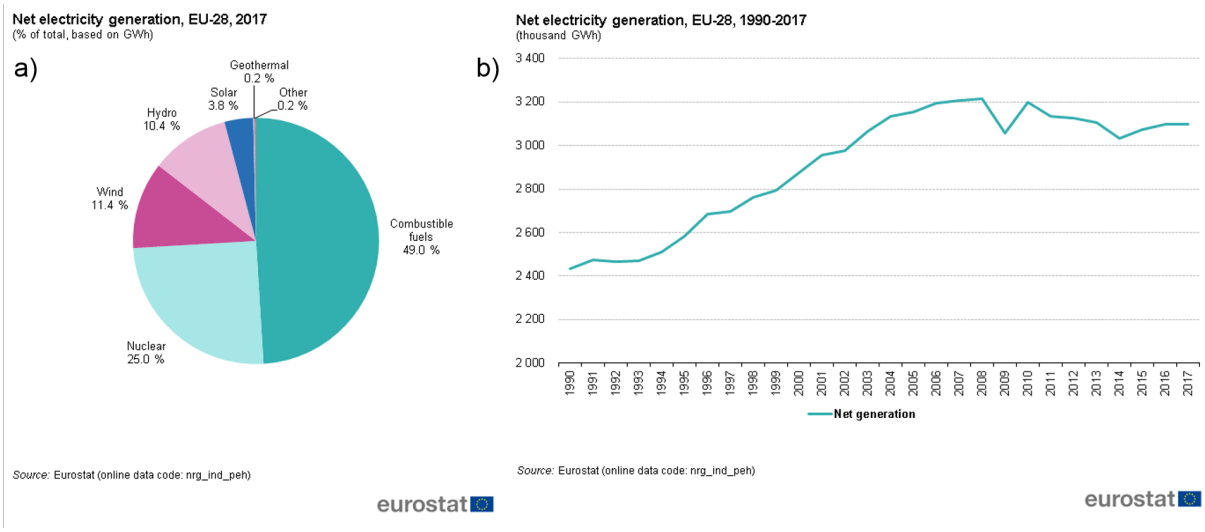

Figure 1.1 a) Electricity mix and b) net electricity production from 1990 to 2017 in the European Union [1].

Figure 1.1 shows that in the EU fossil fuels still provide for half of the Union electricity. In figure 1.1(b), the variation of the electricity generation during the last 30 years can be seen, this curve had a significant growth during the 90s and the start of the millennium to be abruptly stopped in 2009 due to the financial crisis. During the last years, the market is slowly getting back into tracks. Historically, GDP and energy production have evolved in a similar way. Nowadays they are partially decoupled due to the focus on efficiency and energy savings policies. Nonetheless, energy consumption will increase as economical growth gets stronger.

During the last years, road transport has consumed a mean value of around 12.5 millions of TJ [2] which equals to 3400 TWh. Currently, this is powered by fossil fuels but it is expected to change as the electric vehicle gets better autonomy and variety, and taxes increase in conventional ones. This will mean an additional load to the electric grid.

Concerning electricity production, future challenges can be resumed as:

- Renewable energies share is increasing due to climate change and social response to it.
- Fossil fuel based electricity generation is being discontinued. A new baseline energy has to substitute coal and fission energy is not an option in most countries due to bad public perception.
- Electricity consumption is meant to grow due to the recovery of the economy and the electrification of industry and transport.

- New energy agents must be non polluting ones.
- In the European context, energy dependence from other countries must be cut as a strategic point.

In this context, nuclear fusion presents itself as a solid ingredient for a future carbon free energy mix, with no CO_2 production, almost limitless fuel and world wide availability. This producer aims to become the so needed alternative to the base line producers as coal. In long term nuclear fusion could become flexible enough to cover a more quick changing demand.

1.2 Nuclear Fusion

Nuclear fusion is a nuclear reaction where two nuclei collide and fuse, producing a heavier element and releasing energy during the process. Energy released is the energy difference between reactants (e.g. D and T) and products (for D and T: He + n) following Einstein $E = mc^2$. The best candidates for a fusion reaction would be elements with low binding energy -energy necessary to maintain the element stability- that fuse into other elements with high energy. In figure 1.2, the binding energy per nucleon of a large sample of elements is shown, this difference in binding energy is reflected in the slope of the curve, therefore the lightest elements would be the preferred elements to fuse.

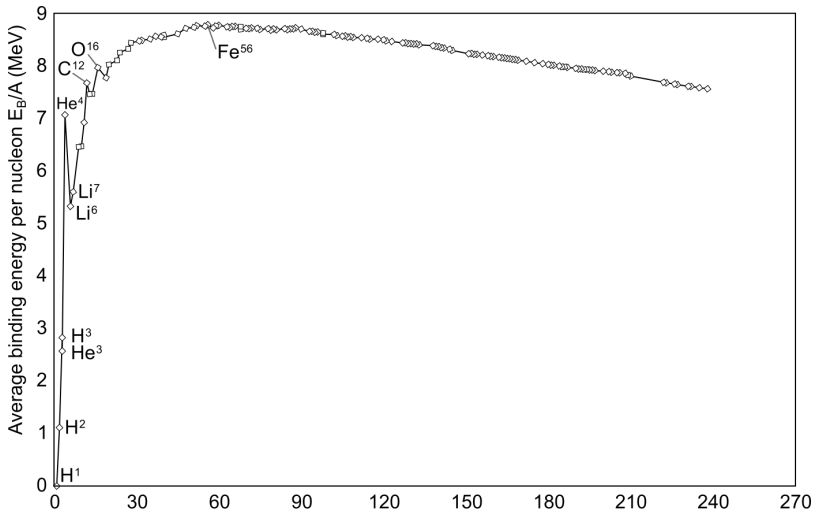

Figure 1.2 Binding energy per nucleon as a function of mass number [3].

Concretely, the largest difference is between He-4 and hydrogen, including its isotopes deuterium (D) and tritium (T). Different reactions have been proposed to achieve fusion: D-D, D-T and D-He^3. According to figure 1.2, the best choice would be the D-D reaction but the released energy of the reaction is not the only parameter to take into account at the time of choosing the correct reaction. Figure 1.3, shows the cross section (the probability of a fusion reaction to occur) as a function of the kinetic energy the involved particles have.

As nuclear fusion is still a research-intensive topic, the D-T reaction is the actual main work line, as it is the reaction with the highest probability to happen and is, as well, the one with lowest energy requirement.

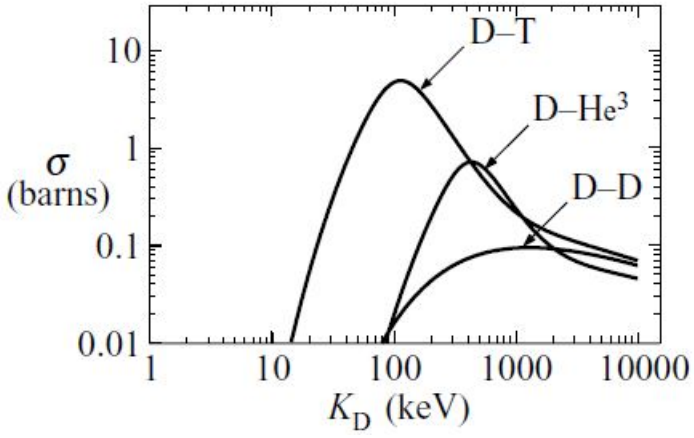

Figure 1.3 Cross section (σ) of different fusion reactions vs kinetic energy (K_D) [4].

The D-T cross section peaks at around 100 keV, which translates into 1000 million K. Achieving this temperature is an engineering feat in its own, but as a reward, this reaction releases 338x10^6 MJ/kg, around 4 times the energy of the fission reaction per kilogram of fuel. Once D-T fusion gets to produce electricity and is well controlled, research will focus in the D-D reaction in order to achieve larger efficiencies. The D-T reaction:

$$D + T \rightarrow \alpha(3.5MeV) + n(14.1MeV) \tag{1.1}$$

There are different alternatives to achieve fusion:

- **Gravitational Fusion:** is the mechanism that takes place in the stars. Fusion occurs due to the immense pressure in the core of the stars, fruit of the huge mass of those celestial bodies. As these weights are not conceivable on Earth, this way cannot be followed to achieve nuclear fusion.

- **Intertial Confinement Fusion:** high intensity lasers are used to bombard a pellet of condensed fusion fuel of around a couple of mm. Each of those lasers are capable of transfering 1 PW in a 1x1 μm^2 area [5] and are distributed symmetrically along the pebble to get a homogeneus heat profile along the pebble. In a few μs, the pebble gets to temperatures of keV and pressure high enough for fusion to occur.

- **Magnetic Confinement Fusion:** a high vacuum chamber is filled with the nuclear fuel, D-T mix or another feasible fusion reaction, in form of gas. It is then heated into an ionized gas, a plasma. D-T plasma is confined through a series of magnetic coils that keeps the fusion plasma from hitting the inner walls of the chamber. When the plasma gets hot enough, particles get enough kinetic energy to overcome Coulomb's

barrier and their collisions can produce fusion reactions. This is, currently, the most advanced of human-made nuclear fusion and will be the design DEMO will be based on, therefore this work will focus on this approach.

In magnetic confinement fusion, once gas is heated enough it becomes plasma, an ionized gas. Commonly, a plasma is defined as:

- **Ionized gas:** high temperatures translate as kinetic energy of the particles involved, once this kinetic energy overcomes the force linking electrons and nuclei, each one can travel freely. So a nucleus will not have anymore a series of electrons around it to compensate its positive charge and vice versa. The ionization temperature for hydrogen is 13.6 eV [6], while fusion requires at least 100 keV as discussed above, so the D-T mix will always appear in plasma form.

- **Quasi-neutrality:** despite positive and negative charges being separated in a plasma, at a macroscopic scale, a plasma appears to be neutral. This occurs because of the formation of Debye spheres (figure 1.4), spheres of neutral charge composed of an ion and a cloud of electrons of equivalent but negative electric charge.

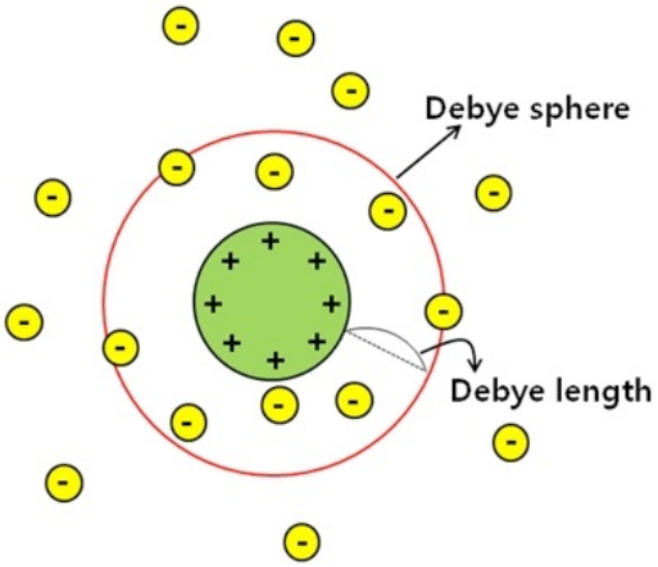

Figure 1.4 An ion is surrounded by electrons forming a electrically neutral Debye sphere [7].

The existence of the Debye sphere creates the concept of the Debye length, that is the radius of said Debye sphere. So, even though plasma is ionized, its behaviour and composition is homogeneous through all space.

- **Collective behaviour:** as the individual effect of any positive ion is shielded by the electron cloud that creates the Debye sphere, the Coulomb forces of single particles won't be the main agent of dynamics inside the plasma. A perturbation that affects a part of the plasma will, eventually, affect the whole system.

- **High electrical conductivity:** the addition of high kinetic energy and low density, due to high temperature, means high conductivity which increases with temperature itself.

1.3 Magnetic confinement fusion and tokamaks

Temperatures of millions of Kelvin are intolerable for current and future materials, therefore fusion plasmas cannot be kept in place through conventional means. The electric nature of a plasma can be used to control its shape and stop it from touching any physical material through a series of magnetic coils.

The first approach for a magnetic confinement fusion device tried to use a linear machine, where a series of parallel coils would produce a cylindrical plasma. But the particles could escape easily from any of the extremes of the cylinder and collide directly with the inner walls of the device, damaging them and losing an important part of the energy of the plasma at the same time.

In 1956 in the URSS, the tokamak (figure 1.5) concept was born. It solved the previous problems by "bending" the tube into a toroidal shape where the particles could travel without getting to a dead end. But this new design brought new problems with it, the coils were not parallel anymore.

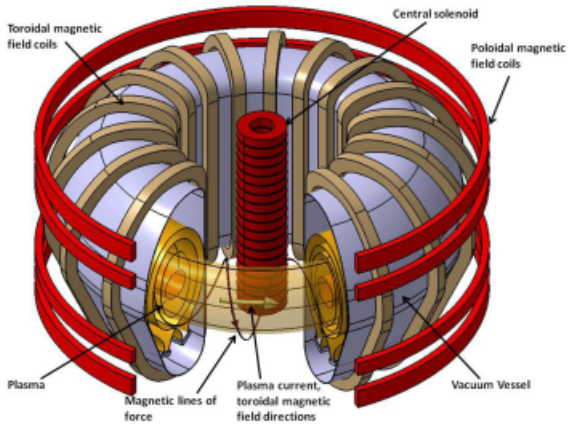

Figure 1.5 Tokamak schematic [8].

This means a magnetic field gradient appears between the inner part of the tokamak -where the coils are closer- and the outer one. The gradient provokes the so-called ∇B drift, which gives a velocity to particles in the perpendicular direction to $\mathbf{B}$ and ∇B [9]. This drift polarizes the plasma, condensing the positive charges on the inner side of the torus and the negative ones in the outer part.

Other drifts exist in a tokamak, one of the most important is the $\mathbf{E}\times\mathbf{B}$ drift (figure 1.7). It appears due to the existence of an electric field perpendicular to the magnetic field. The

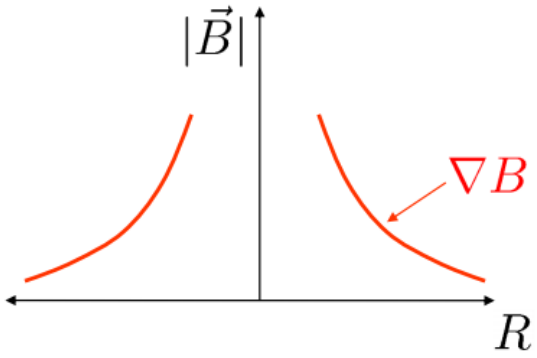

Figure 1.6 Magnetic gradient through the radius axis due to the growing distance between coils [10].

resulting movement displaces the particles to the exterior of the tokamak.

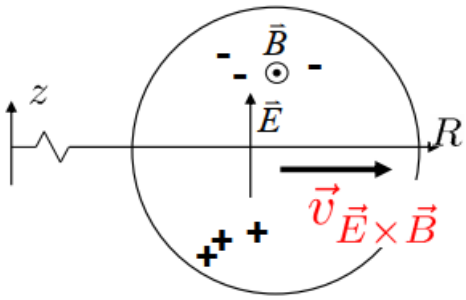

Figure 1.7 $\mathbf{E}\times\mathbf{B}$ drift. Positive and negative charges got the same motion [10].

The separation of charges and the gradient of density resulting from both drifts are serious problems that must be taken into account. The tokamak design tackles them by adding a central solenoid and a series of poloidal magnetic field coils (figure 1.5) that create a toroidal current which twist the magnetic field, compensating the drifts in the process.

This is not the only approach in magnetic confinement fusion to the drift issue. In 1950, in the UK the stellarator design (figure 1.8) was conceived as a first solution for the necessary B twist. The stellarator design avoided the addition of the central solenoid by reshaping the magnetic coils and can currently get plasma pulses of several minutes while most tokamak can only achieve a few seconds. The reshaping of the coils meant an important engineering challenge as each coil was meant to be different and with intricate numerically-obtained geometries. At the same time the toroidal symmetry was broken as the magnetic field in each poloidal face was now different, which makes simulating and working with this type of device more challenging than a tokamak. These reasons have made the ITER project (the largest fusion facility ever built) to follow the tokamak design over the stellarator.

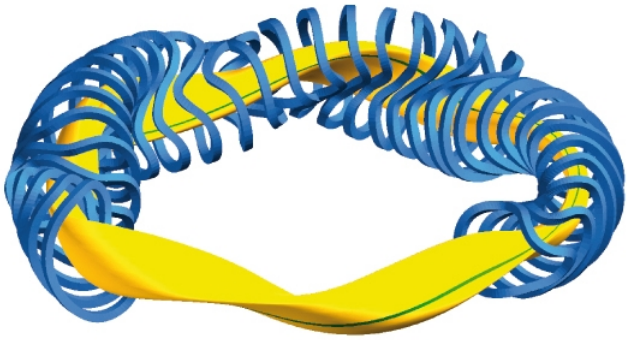

Figure 1.8 Visualization of the coils (in blue) and plasma (in yellow) of Wendelstein 7-X, biggest stellarator in the world. Located in Greifswald, Germany [11].

1.4 ITER and DEMO

In 2006, the ITER project started its construction in France. ITER is an international project lead by the European Union, with the goal of building a tokamak capable of demontrating the feasibility of obtaining positive net energy from a fusion device, in this case, ITER is aiming to get 10 times the input energy. ITER focus is not producing electricity from nuclear fusion power but demonstrate that the current understanding of physics and engineering are ready to overcome the landmark of net positive energy and to take the next step in the fusion roadmap, DEMO, the first fusion reactor to produce electricity and become self-sustained. [12]

As no electricity will be produced from ITER, there won't be any power production cycle associated to it. All the heat ejected by the fusion reaction will be dissipated by a water cooling system. In general, current tokamaks don't need a cooling system as the plasma discharges are short enough (a few seconds at best) that, with some good operation practices, the device and its diagnostics should not receive thermal induced damages. But ITER is aiming at plasma discharges of around half an hour with heat fluxes on the order of 1 MW/m^2, no material could withstand such temperatures and, therefore, a cooling system is necessary.

Tritium needed for the D-T reaction is almost non-existent in nature due to a short half-life of 12 years. Currently, tritium is produced as a by-product of CANDU fission reactors. ITER will make use of the existing reserves of tritium for its operation. DEMO aims to produce its own tritium by featuring a breeding blanket able to convert lithium into tritium through a nuclear reaction. This topic will be further discussed in section 2.3.

The scope of DEMO is to achieve electricity production and its preliminary design reflects it. While ITER vessel is fully covered with ports for diagnostics (figure 1.9), in DEMO the number of ports is minimized to reduce asymmetries, disruptions and complexity of the device. The mission of DEMO is not physics research but power production.

The parameters of ITER and DEMO are summarized in table 1.1.

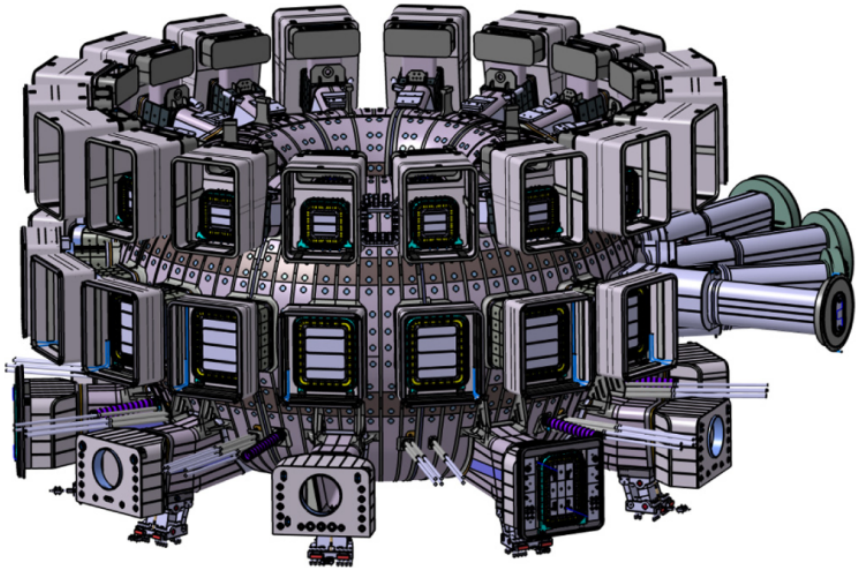

Figure 1.9 ITER vessel with the ports needed for diagnostics [13].

DEMO requires a power plant to transform its heat production into electricity. Different designs have been proposed, a classic Rankine cycle similar to the ones used in nuclear fission, a proved technology in the nuclear field [14], [15]; a Brayton cycle based on helium to take advantage of its resistance to radiation [16] or a supercritical CO_2 Brayton cycle, able to reach high temperatures and, therefore, high efficiencies [17], [18]. In this thesis a supercritical carbon dioxide (S-CO_2) cycle will be studied.

1.5 Motivation

Nuclear fusion that can get us cheap and clean electricity is a dream that has been chased since World War II. Nowadays, this dream is more needed than ever. The lack of energy sources in European soil and the threat of the imminent climate change have taken the EU agenda to gravitate towards the research and construction of new reactors and experiments that can take the scientific community to achieve this objective.

As part of this effort the ITER project is under construction with international collaboration and, in parallel, the European Union is drafting what will be the first fusion power plant in the world, DEMO. Currently, the DEMO project is in the conceptual design phase and this work is framed in this space. The goal is to propose new layouts for a DEMO like power plant based on a Brayton supercritical carbon dioxide cycle.

Using supercritical CO_2 continues with a research trend that is exploring the capabilities of these types of cycles and that is expected to grow considerably in the next years. Said capabilities are already being studied in the fusion framework and this work is expected to continue this line.

Table 1.1 Main parameters of ITER and DEMO [19].

ITER	DEMO
Experimental device with physics and technology missions	Nearer to a commercial power plant, but with some development missions
400 s pulses (some longer at lower power), long dwell time	Long pulse, quasi-steady state
Experimental campaigns. Outages for maintenance and component replacements	Maximize availability
Large number of diagnostics	Only those required for operation
Multiple heating and current drive systems	Fewer
Large design margins, necessitated by uncertainties and lack of fully appropriate design codes	With ITER (and other) experience, design could have smaller uncertainties
Cooling system optimized for minimum stresses and sized for modest heat rejection	Cooling system optimized for electricity generation efficiency (e.g. higher temperature)
Test blanket modules introduce range of diverse concepts	Single blanket concept
Unique one-off design optimized for experimental goals within cost constraints	Move towards design choices suitable for series production
No tritium breeding requirement (except very small quantity in TBMs)	Tritium breeding needed for self-sufficiency
Conventional 316 stainless steel structure	Novel low activation materials as structure (at least for some components)
Very modest lifetime neutron fluence, low dpa and He production	High fluence, significant materials damage
Licensing as experimental facility allows some credit for experimental nature (e.g. no dependence of safety on plasma behaviour)	Stricter approach may be necessary to avoid large design margins
During conceptual design (including "EDA"), licensing in any ITER member country had to be possible	Fewer constraints

2 DEMO description and typology

DEMO has already been introduced as the next step in the European roadmap to fusion after ITER proves the feasibility of nuclear fusion as an energy producer. In this chapter a description of the general topology of DEMO and the different designs under development will be presented. Next, the available heat sources will be discussed in terms of the possible output power and achievable temperature. The current version of DEMO, the DEMO Baseline 2018 is introduced and the code used to obtain it, PROCESS, is presented.

DEMO is the name given internationally to the next step after ITER. This power plant will not be a global effort as ITER, each country or group of countries is working on their own unique design. Only the European DEMO will be in the scope of this work.

2.1 DEMO topology

In this section a description of the general structure of DEMO will be given, explaining at the same time the parts that compose a tokamak (figure 2.1) and the particularities that define DEMO:

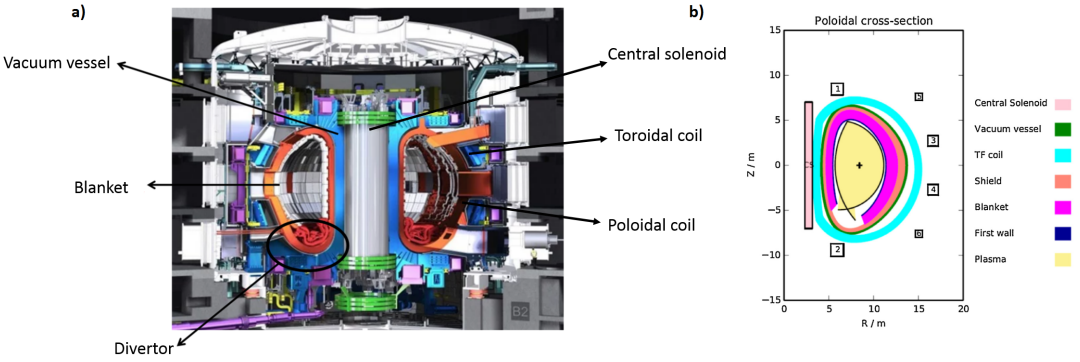

Figure 2.1 a) 3D render of an ITER section [20]. b) Schematic with most important DEMO parts [21].

- **Magnetic field coils:** two kind of magnetic field coils are used in tokamaks. Toroidal field coils, focused on producing a toroidal magnetic field. And poloidal field coils, which through the variation of its current are able to shape the plasma. Normally, the plasma presents a D-shape with a X-point formed by the intersection of the last closed flux surface (LCFS). This structure provides a longer lasting plasma and lets the plasma eject the impurities that may appear during operation. DEMO is expected to use superconductors for the coils with active cooling with the objective of achieving 20 T peaks [14]. Cooling will be done with helium as temperature of just a few Kelvin are necessary for the good functioning of the coils.

- **Central solenoid:** is the primary winding of a transformer with the plasma itself being the secondary. The central solenoid inducts a current in the plasma which is essential for the existence of the plasma. In order to maintain the plasma current, the current of the central solenoid has to keep a constant growth. But the current of the central solenoid cannot grow endlessly. When the current saturates, the plasma will start to lose stability and, eventually, will shut down. The central solenoid saturation current marks how long a plasma discharge lasts.

  This barrier could be overcome by replacing the central solenoid current by the bootstrap current. The bootstrap current is a self-induced current created by the plasma due to the transport of electrical particles inside it [9]. Current tokamaks have only produced a fraction of the needed current through this mechanism, the stationary design of DEMO (DEMO 2) foresees that a machine of its size and characteristics could produce a high enough bootstrap current to not depend of the central solenoid apart from the start up of its operation.

  A second important task is charged onto the central solenoid, heating the plasma. The induced plasma current heats up the plasma as a result of the Joule effect. This effect gets weaker as the temperature increases because plasma resistivity decreases with temperature. So other means have to be put in play for further heating such as NBI (Neutral Beam Injector) or ECRH (Electron Cyclotron Resonance Heating).

- **First wall:** constitutes the first plasma envelope. In DEMO the layer that directly sees the plasma is called *armour* and is made of thin tiles of less than a centimeter of tungsten. Tungsten has been chosen due to the capability of the material to withstand the expected thermal loads of 3-5 MW/m^2. This heat flux flows to the rest of the structure through conduction and from there is cooled thanks to a myriad of cooling pipes. Helium, rather than water, has been chosen as the preferred coolant because it can get to higher temperatures and there is no risk of activation due to reactions with the incoming neutrons from the plasma (equation1.1).

  A sudden rise on the temperature in the first wall, i.e. due to a disruption, can burst the cooling pipe producing a Loss Of Coolant Accident and forcing a stop in the normal DEMO operation. This can be avoided with thicker armour tiles, but thicker tiles will capture more neutrons, reducing the electrical output of the plant as less heat will arrive the blanket. A compromise solution has to be set in order to get a balance between security and profitability.

- **Breeding blanket:** the next layer after the first wall. In an ideal situation it is where all neutrons will collide and release its energy. This is where the tritium production takes place ("breed"). The main material of this region is some lithium based compound, which one depends of the chosen design. The reaction of Li with a neutron produces tritium as shown in equation 2.1. The self-sufficiency of tritium in a fusion power plant is essential as tritium is almost impossible to find naturally due to its short half-life.

$$^{6}\mathrm{Li} + \mathrm{n} \longrightarrow {}^{4}\mathrm{He} + {}^{3}\mathrm{H} \tag{2.1}$$

  A good cooling system is needed as most of the energy will be deposited in this layer. DEMO options for cooling are water o helium pipes or, as an advanced option, using liquid lithium as breeder and coolant at the same time.

  DEMO will be the first tokamak to have a complete breeding blanket, previous tokamaks have regular blankets with no tritium production and ITER will be the first to feature a breeding blanket module, but just for testing purposes.

- **Vacuum vessel:** is the last frontier with the exterior. Its main mission is to maintain the sealing of the reactor. In between the blanket and the vacuum vessel is the shield, an intermediate layer that reduces the amount of neutrons that get to the vacuum vessel to the minimum.

- **Divertor:** during operation, different impurities start to appear inside the plasma (e.g. metals from the walls erosion). High impurities level can cause plasma stability problems, therefore a mechanism to pump out the impurities has to be put in place. Through the action of the magnetic coils, the LCFS is set to have a shape with a couple of "legs" that collide with the lower part of the tokamak in the so called divertor. Impurities eventually gets to the divertor where they are extracted from the tokamak. The divertor is where the highest heat fluxes (in the order of 10 $\mathrm{MW/m^2}$) are to be expected, as there is a direct contact between plasma and divertor, so cooling is mandatory.

  DEMO will have only a lower divertor, cooled with water or helium depending on the final design.

2.2 DEMO 1 and 2

Until 2027, DEMO will be immersed in the conceptual design phase. Currently two major designs are been evaluated, a pulsed design, DEMO 1 and a stationary one, DEMO 2 [22].

DEMO 1 is the most conservative design, based on technology and physics well known and established. It will be a pulsed design, due to the saturation current issue of the central solenoid, as this is the current mode of operation. Biggest tokamaks at the moment have pulses of several seconds, ITER is expected to pulse for 30 minutes and DEMO 1 is being

designed with 120 minutes long discharges with 30 minutes of dwell time [23]. These 120 minutes time only account for the stationary time, ramp up and down are not included.

A pulsed operation means a series of issues for materials and equipment involved as they will be affected by cyclic loads. This is especially important for the turbine of the power cycle, to mitigate this situation thermal energy storage (TES) can be included in the power cycle.

DEMO 2, on the other hand, looks for a more optimistic design where it can work continuously only getting stopped by maintenance or emergency stops. This can only be achieved if the bootstrap current and external power are able to sustain the plasma. To this end, improvements in the physics and engineering fields have to take place before the final design is chosen. This type of reactor will be superior to DEMO1 as its availability will be inevitably higher, it won't have the energy consumption related to the central solenoid and its components won't suffer from cycling loads.

The current official baseline (2018 baseline at the time of this writing) focuses on the DEMO 1 pulsed design. DEMO is a critical point for the European fusion roadmap and will use as much known technologies as possible.

2.3 DEMO breeding blanket

Due to the novelty of a breeding blanket and its importance for a self-sustained operation, four different designs have been carried out by EFDA (European Fusion Development Agreement). Each design features a more advanced design, with higher operating temperatures and larger bootstrap current fractions. The first two schematics are meant for a near-term DEMO and the later two, for a scenario where DEMO has to be built quite much later or the engineering and physics research has improved faster than expected [24], [25], [26].

- **Water-cooled lithium-lead:** or WCLL or Model A. Uses water to cool the blanket and the divertor. As water is the main heat transfer fluid used in power production, its advantages and problems are widely known making this design the most conservative and easy to achieve. On the other hand, water will not translate the in vessel high temperature to the power cycle due to a relatively low maximum working temperature. A low-activation martensitic steel is needed as structural material due to the high neutron bombardment it will suffer. Current accepted option is EUROFER 97 that achieves the low-activation requirement at the cost of a maximum temperature of 550ºC [27].

  Lithium is used as the breeding material following equation 2.1 and lead as neutron multiplier. Having a neutron multiplier is necessary to keep the system self-sufficient, a fusion reaction only produces one neutron which would be needed for tritium breeding to keep the balance on point, but some of the neutrons stop before getting to the breeding blanket or just pass through it without hitting the lithium. Therefore a neutron multiplier is mandatory to sustain the reactions.

An alternative version that exchanges water with helium, HCLL, is also proposed as Model AB [27]. Even though water can evacuate 1.5 MW/m^2 versus 1 MW/m^2 in the case of helium [28], helium can get to higher temperatures and will not be affected by radiation of neutron bombardment.

- **Helium-cooled pebble bed:** or HCPB or Model B. Breeding blanket is now composed by layers of lithium with pebbles of beryllium. Lithium will be used as tritium generator and beryllium as neutron multiplier. This second design is cooled by helium which can get to higher temperatures thus higher thermal efficiencies in the power plant. EUROFER 97 will be still used as structural material but plasma facing walls (divertor, first wall) require material that can withstand larger temperatures.

- **Dual coolant blanket:** or DCLL or Model C. Lithium-lead is used again as breeder and neutron multiplier respectively. Cooling is carried out by both helium and LiPb. The cooling loop associated with LiPb can get to temperatures of 700ºC.

- **Self cooled blanket:** or Model D. LiPb works as coolant, breeder and neutron multiplier. Using a single fluid means a simpler balance of plant and unifies the pumping system. Here, the structure is designed to be made out of silicon carbide composite [26] which lets the coolant get to around 1100ºC.

Among these 5 designs, WCLL and DCLL have not seen many research efforts as they are seen as inferior versions of HCLL and Model D [27]. HCLL and HCPB are recognized by EFDA due to “have considerable safety, environmental and economic potential” [26]. The HCPB design is the chosen design to represent the DEMO Baseline 2018 during this work.

2.4 Heat Sources and DEMO 2018 Baseline

DEMO general structure and design have already been described. Next step is to define and dimension the available heat sources. For this, the DEMO 2018 baseline will be used. First, the mechanisms of heat transfer that take place in a tokamak must be explained, these are summarized in figure 2.2.

Values shown in figure 2.2 are not the exact same of the 2018 baseline but an approximation of what a fusion reactor could look like. The figure show the path heat takes, being the starting point the external heating (58 MW) and the power generated by the fusion reaction (2300 MW). As expected, 20% of the fusion power is in form of α particles (460 MW), which keep the plasma hot, but in the process 2% of it is lost (10 MW). Adding external heating and alpha particle power means that the plasma is heated with 508 MW. The plasma radiation supposes 120 MW that is distributed in 110 MW to the first wall and 10 MW to the divertor. The rest of the plasma power goes to the scrape-of-layer (SOL), the plasma surface, most of this power is evacuated through radiation (363 MW) and the rest is cooled by colliding with the divertor plates (25 MW).

The remaining 80% of the fusion power is present in the form of kinetic energy for the

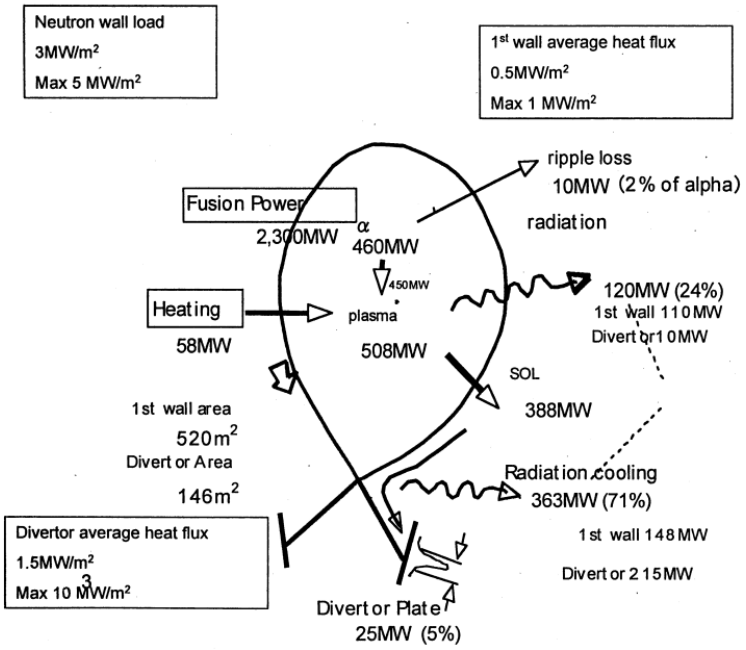

Figure 2.2 Heat distribution in a tokamak [14].

produced neutrons. These neutrons will collide with all the layers of the reactor; first wall, breeding blanket and shield.

The PROCESS code [29] (discussed in chapter 2.5) has been used to determine the DEMO Baseline 2018. This baseline is constrained as a 500 MWe power plant with a HCPB type breeding blanket with water cooled shield and divertor. The figure of merit of the optimization problem is *rmajor*, plasma major radius. The resulting physics and engineering parameters constitute the DEMO Baseline 2018. From this baseline the expected usable heat from the different sources are obtained:

- **Breeding blanket and first wall**: main power source of the tokamak, limited to 500ºC due to using a breeding blanket Model B (a 50ºC security buffer has been added). The power received in the first wall through radiation and collisions, power in the breeding blanket due to thermalization of neutrons and released by the tritium breeding reaction which is exothermic (4.8 MeV [30]), extra power due to neutron multiplier and, lastly, the combine losses all the previous elements are combined in this source. Along this work, this set of power will be denominated as breeding blanket power as this is the main power source of both. The power in blanket and the first wall is: **2254.026 MWt**.

- **Divertor**: even though it should be the source with the highest temperature output, it is capped at 150ºC in the DEMO baseline because it is meant to be cooled by water. The power in the divertor is: **389.493 MWt**.

- **Shield**: similar to the divertor, it is water cooled, so its outlet temperature can't be higher than 150ºC. In this case the effect of the low temperature on the efficiency is not as dramatic as in the divertor because the total power is quite low in relative

terms. The power in the shield is: **1.483 MWt**.

Table 2.1 Electric power needs for DEMO in Baseline 2018.

Heating and current drive	127.5 MW
Primary coolant pumps	234.0 MW
Vacuum pumps	0.5 MW
Tritium plant	15.0 MW
Cryoplant	39.9 MW
Toroidal field coils	9.5 MW
Poloidal field coils	0.6 MW
Other internal electrical power requirements	64.816 MW
TOTAL	**491.9 MW**

For a fusion reactor to work, a lot of devices must be fed with electric power. These consumption will tax the electric power coming from the power cycle and, therefore, are accounted when determining the final electricity generation and the efficiency of the whole system. In table 2.1 the electric needs for a fusion reaction defined by the DEMO Baseline 2018 are presented.

2.5 PROCESS basis

PROCESS is a system code developed by the Culham Centre for Fusion Energy (CCFE) as part of the UKAEA (United Kingdom Atomic Energy Agency). This code aims to give a wide and coherent view of a fusion reactor with an associated power plant. PROCESS is divided in two strongly dependent modules, one focused in the physics of the reactor and another on its engineering [31], [21].

In the physics module, the main objective is to simulate plasma according with the chosen boundary conditions, for this a good definition of the magnetic field inside the tokamak is needed and calculated inside the tool. The magnetic field will be the result of the position, material and magnetic field of the poloidal and torodial coils, together with the contribution from the plasma itself. As an additional input to get the plasma parameters (plasma geometry, density and temperature profile, emissivity, current density...), heating systems must be added. These heating systems have to be geometrically placed in the tokamak and its characteristics specified. PROCESS can use neutral beams, electron cyclotron heating and current drive. Knowing the magnetic field and the heating systems, plasma parameters are calculated [31]. Note that this is an iterative problem as the resulting magnetic field must satisfy the physics and engineering constraints introduced by the user. As those parameters have already been defined in the European DEMO Baseline 2018 and they are not in the scope of this work, they will be defaulted to the Baseline values.

From an engineering point of view, the code excels in two fields [21]: coils characterization and usable heat power balance. Again coils and heat balance appears in this

module, but they will be observed under a different scope. This time coils will be studied by themselves focusing on the feasibility of building those coils, therefore the stresses are estimated as well as the current density in said coils. This will be studied not only for the poloidal and toroidal field coils but also for the central solenoid.

If in the physics block the heat balance was about what enters into the plasma, the engineering one treats the power fluxes coming from the plasma and the electricity needed to keep the plant as a whole working. PROCESS divides the usable heat sources in divertor, first wall, blanket and shield. Heat is divided in primary heat, highly exergetic heat, and low-grade heat (LGH), that is not usable and has to be evacuated. Figure 2.3 shows the heat fluxes through a fusion power plant.

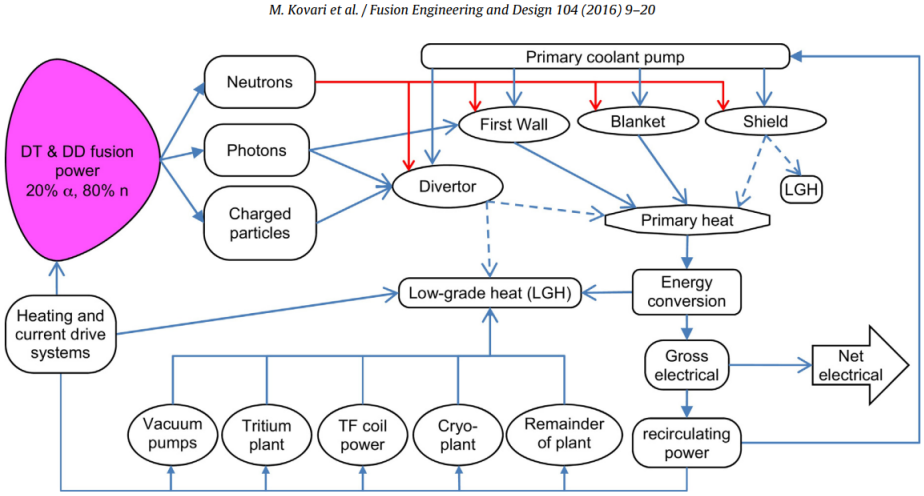

Figure 2.3 Heat balance in PROCESS. Dashed lines represent different options [21].

Electricity needs of the whole plant and the availability are also calculated, which will be essential to calculate the cost of electricity (COE). PROCESS features a third optional module about plant cost and COE. In this module construction, machinery and other installation costs are estimated, giving an overall estimation of the total cost of a fusion power plant. In this module the COE is also calculated, this parameter is important to compare nuclear fusion with other energy sources and to check the profitability of a fusion power plant. As fusion energy is not even a power producer yet, COE is expected to be higher than current energy sources that have been industry-ready for a long time.

2.5.1 Running PROCESS

The PROCESS code is able to solve non-optimisation problems using the HYBRD method [32], this non-optimisation mode was used to explain the direct problem at the beginning of this section (knowing the machine, the resulting plasma, coils and heat balance are resolved). Figure 2.4 shows the work flow during a non-optimisation case. However, the main strength of PROCESS comes from the resolution of optimisation and parametric

problems with numerous constraints with the VMCON subroutine [33].

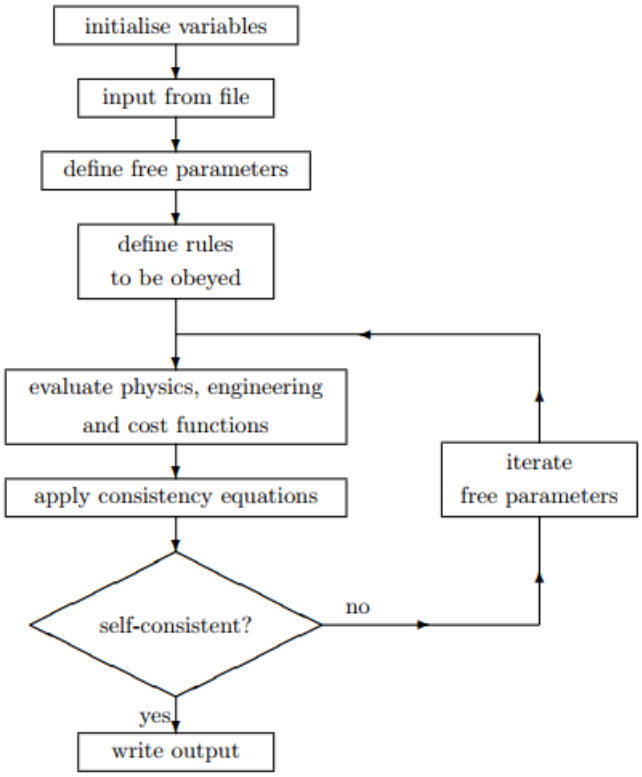

Figure 2.4 Flow diagram of PROCESS in non-optimisation mode [34].

Normal operation in PROCESS is the optimization mode, the other different operation modes are extra additions to the code to make it more flexible. The goal of the PROCESS solver is to get the auxiliary parameter $c_i = 0$. With this goal in mind, equations in PROCESS can be divided in two types: consistency equations and limit equations. [34].

Consistency equations keep the engineering and physics consistency of the whole model. It ensures that any two equations h and g are equal:

$$c_i = 1 - \frac{g}{h} \tag{2.2}$$

The solver will try to get $c_i = 0$, therefore making $g = h$.

Limit equations are inequalities coded as an equality with a coefficient f varying between 0 and 1. This can be used for upper (eq. 2.3) and lower (eq. 2.4) limits:

$$c_i = 1 - f * \frac{h_{max}}{h} \tag{2.3}$$

$$c_i = 1 - f * \frac{h}{h_{min}} \tag{2.4}$$

As c_i converges to zero, the value of h will be at a certain distance (defined by f) of the superior or inferior limits set.

The user must input which equations are going to be solved from a list that can be found in the code documentation or in the User Guide [34] and the parameters that will vary to optimize the problem. In PROCESS each parameter, equation or figure of merit is identified by a number. Finally, a figure of merit must be chosen from the available ones, if it is to be minimized it will be left as a positive value and negative if it is a maximization problem.

For further information on how to run PROCESS refer to the User Guide [34] available in the CCFE website.

2.6 European DEMO Baseline 2018

As part of the European effort to achieve commercially available nuclear fusion, different teams are working in a wide range of topics, from the physics basis of plasma to state-of-the-art material science. For all those teams and institutions to work with the same goal machine in mind, the EU creates the European DEMO Baseline that sets a common ground to work with. Current official version is the European DEMO Baseline 2018 that was developed using the PROCESS tool. This Baseline will be used as the basis for a pulsed reactor scenario (DEMO1), as it contains the available power from each heat source as well as their constraints. Also, the consumption of the reactor and its auxiliaries are obtained from this Baseline. It will serve to correctly estimate the net electric production of the whole power plant.

The European DEMO Baseline 2019 is also available but as it is not the official version yet, it will not be used.

3 Supercritical CO_2 for a fusion power plant

For this work, a supercritical CO_2 (S-CO_2) Brayton cycle has been chosen as basis for the power plant. In this section, this choice will be justified, explaining the benefits and problematic of these new type of power cycle and describing the current research line on this topic.

3.1 Supercritical CO_2 in Brayton cycles

Carbon dioxide is a common substance, 0.03% of the atmosphere is CO_2 and is a product of any oxidation reaction with carbon. Nowadays, CO_2 is one of the main agents provoking the greenhouse effect, not due to its greenhouse potential, but due to its abundance and the large production derived by an economy based on carbon. There is a current trend on reducing CO_2 production or even capturing it to meet the emission limits set by the governments and to improve the public image of business historically seen as great polluters.

The critical point for carbon dioxide is set at 73.77 bar and 30.98ºC. So a power plant using this fluid must work at high pressure along the whole cycle to maintain supercritical conditions. For this reason, and given its simplicity and compactness, the Brayton cycle is the most extended choice when studying S-CO_2 for power production. Brayton cycles are commonly used to produce electricity out of the combustion of gas. This cycle (depicted in figure 3.1) works following these processes [35], [36]:

- Point 1 refers to the compressor inlet, with clean air at ambient pressure and temperature.
- From point 1 to 2, air is compressed isentropically (if the process was ideal).
- Compressed air enters the combustion chamber where gas is burnt at almost constant pressure (point 2 to 3). The resulting mix of air and combustion gases are then in a hot, high pressure state (point 3) that is expanded in a turbine to generate a mechanical

torque that will power a generator which produces electricity. The exhaust gases of the turbine (point 4) are then released into the environment.

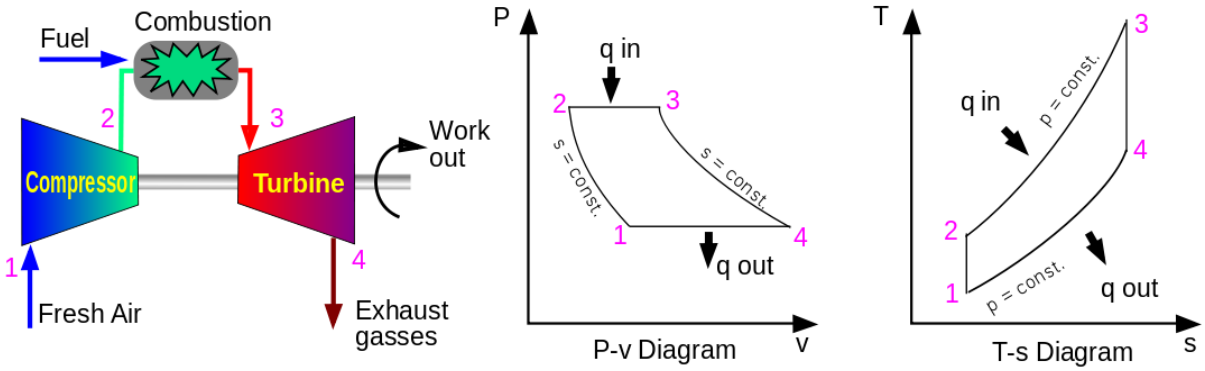

Figure 3.1 Different representations of a Brayton Cycle, from left to right: Gas turbine block diagram, pressure-volume and temperature-entropy [37].

The S-CO_2 cycle is characterized by:

- It operates in a closed cycle. Carbon dioxide at the turbine outlet is not released into the environment, it is cooled before entering the compressor.
- Heat is provided by an external source (for a fusion power plant case, heat sources were described in section 2.4) and the working fluid is cooled through heat exchangers.
- Inlet condition of compressors are above carbon dioxide supercritical conditions, 73.8 bar and 30.98ºC.

Figure 3.2 shows the supercritical carbon dioxide in a temperature-entropy diagram, where the temperatures at the compressor and turbine outlet are indicated. The temperature in point 4 turns out to be around 200ºC higher than at point 2. This means that a regenerator can be added using both streams to decrease the necessity of external heat between 2 and 3. Also, the cooler would need to be smaller as some of the previously evacuated heat is now kept into the system. In general, this means a higher efficiency and less equipment cost (despite adding a new heat exchanger).

This benefit increases as a the inlet temperature to the turbine becomes larger. In a future power plant, where extremely high temperatures are expected, this can be translated into important regeneration processes that can improve the efficiency of the power cycle. In the current baseline the temperature has been limited to 500ºC due to materials problems in the supporting structure, as presented in chapter 2.4. However, once the material problems get solved and higher temperatures become achievable in the primary coolant, this positive effect will have a larger weight on the efficiency of the whole power plant.

In the gas turbine, compressor consumes 1/3-1/4 of the total power delivered by the turbine. However, in the S-CO_2 cycle, with the compressor operating close to the critical point supercritical carbon dioxide behaves partially as a liquid and the work required to

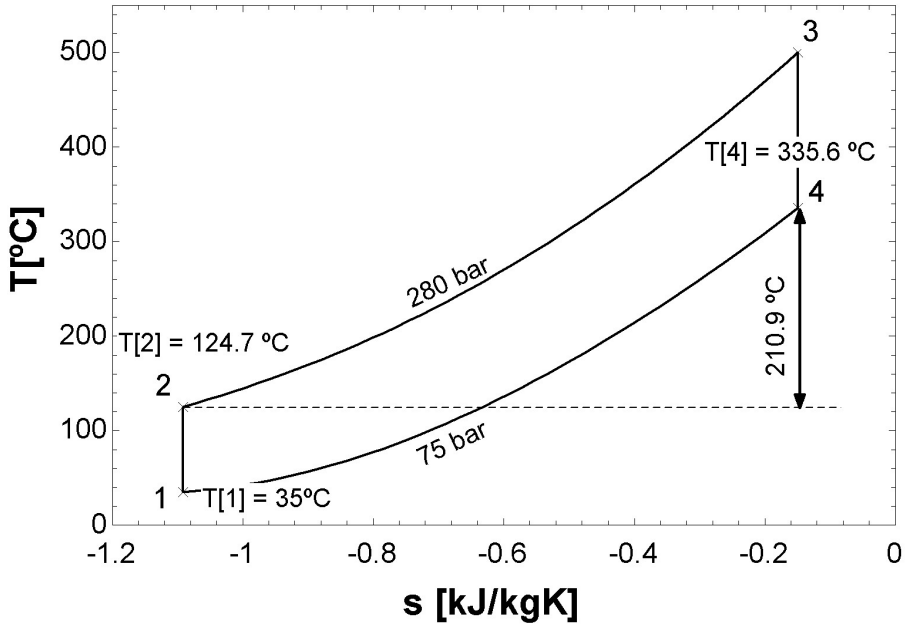

Figure 3.2 Temperature-entropy diagram of S-CO_2 cycle. The large temperature difference between point 2 and 4 gives the opportunity of regeneration..

compress it is not that high anymore. This phenomenon is visualized in figure 3.3, where the power required to duplicate the pressure for different temperatures and starting pressures close to the critical point are shown.

When the pressure is low enough, carbon dioxide behaves like a gas and the power required is increased, but this situation is reversed as the pressure grows and a minimum appears on the required work. Unfortunately, this minimum is very sensible to the chosen temperature. For an optimum pressure, just increasing one degree can mean entering into the gas zone. Therefore, one must renounce on working on that point or be sure to develop a robust enough control system to keep that point fix.

With an adequate design and control of compressor inlet temperature the required size of the compressor and gas turbine would be of a reduced size. However it implies the cooling of the compressor inlet and the associated parasitic consumption. The optimal option will be the result of the balance of the different requirements and definition of the operation modes. This means savings on equipment and layout space. A very important advantage of the use of the S-CO_2 Brayton cycle over, for example, a Rankine cycle is the tritium recovery. Some of the tritium produced in the blanket is expected to leak into the primary coolant cycle and from there, into the power cycle. This will require a treatment plant that extracts the tritium from the CO_2, and this extraction is easier to complete from CO_2 than from water [38].

The control of heat exchange with the S-CO_2 is an issue. Due to the shape of the temperature heat transfer curve of CO2, the minimum difference of temperatures, pinch point, can happens inside the heat exchanger (figure 3.4), complicating the design of an

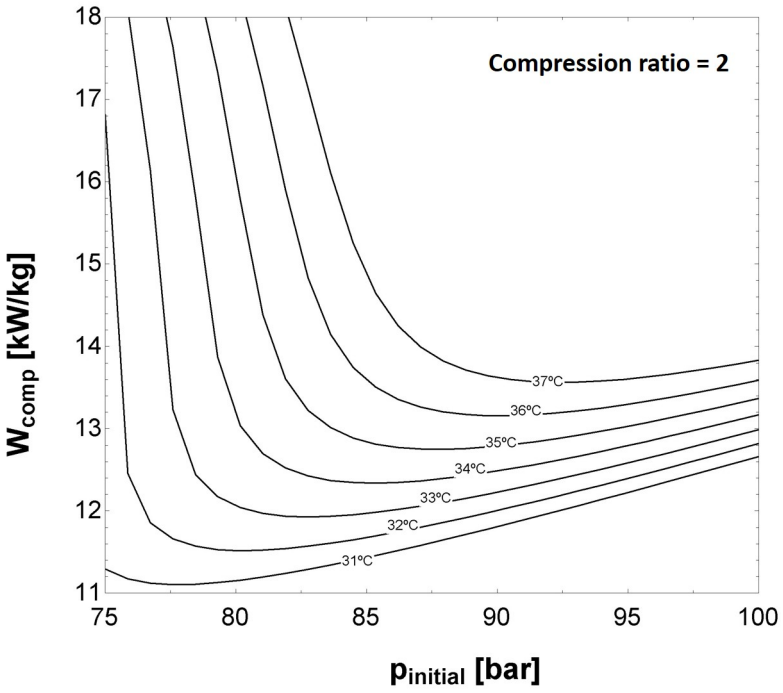

Figure 3.3 Power required for a compression ratio of 2 near the critical point for carbon dioxide.

effective heat exchange system and control. The pinch temperature must be enlarged if the pinch point is violated inside the device. For this, a careful analysis of the evolution of the temperature in the device must be done.

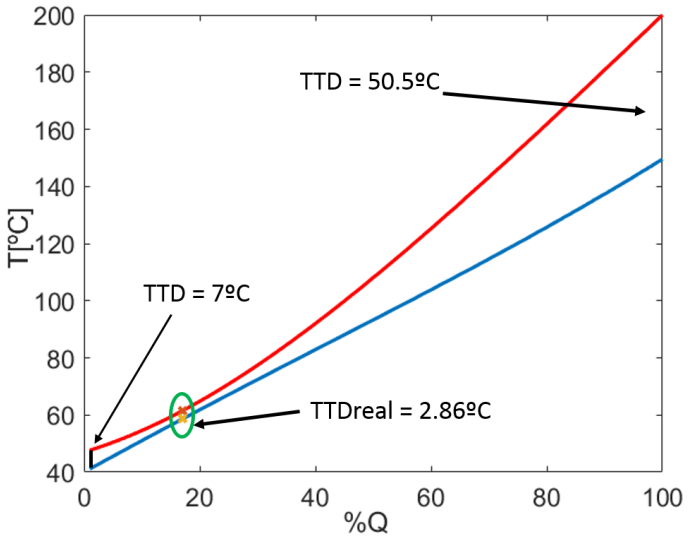

Figure 3.4 T-Q diagram of a heat exchanger working with supercritical CO_2 the minimum pinch temperature is not at the extremes of the heat exchanger but in an intemediate point.

3.2 Past and current research on supercritical carbon dioxide

In 1948, Sulzer Bros. [39] first introduced the benefits of working with S-CO_2. It wasn't until 1967 when Feher gave their current name to this working region, supercritical carbon dioxide. In this publication [40], Feher started to point out the problematic of the pinch point explained in the previous section. These discoveries started a first boom in the research of S-CO_2, highly motivated by the novelty and the first results, that showed high efficiencies.

During the 1960s and 70s, the S-CO_2 cycle was proposed as as alternative to common power cycles for power production from nuclear plants [41], [42] . Feher, in 1970, built a first test generator using S-CO_2 for a nuclear reactor [43], this was supported by previous papers [41] that defended that a single heating cycle using this substance could outstand over a reheat Rankine cycle. However, S-CO_2 didn't score well in the Energy Conversion Alternatives Study (ECAS) carried out by General Electric in 1976 studying the suitability of this cycle and substance, among others, for conventional fossil power plants. And as carbon-based power plants were the norm for the next decades, S-CO_2 research was kept in a drawer awaiting for a change.

With the new millennium, new opportunities emerged. Technology restrictions that stopped the appearance of power plants based on supercritical carbon dioxide had been overcome: compact heat exchangers, increased knowledge on turbomachinery [44]. In addition, new power sources appeared, like concentrated solar power with salt-based energy storage [45] or liquid metal reactors, and the economic, environmental and political push for better efficiencies helped the reborn of supercritical carbon dioxide in the industrial and scientific scene.

Other uses not related to electricity generation have been found for S-CO_2. In 1977, Combs proposed its usage for naval propulsion thanks to its compactness and fuel savings [46], it has found a niche of work on chemical extraction of substances [47] and in waste heat recovery [48].

Currently, supercritical carbon dioxide has strongly recovered the interest, Crespi enumerates ten important test facilities distributed all around the world [49] and makes a systematic review of the current scenario. His paper counts 42 stand-alone cycles, 38 combined cycles and another few classified as "other" cycles. Especially relevant for this work is the presence of S-CO_2 for a DEMO-like power plant design. As it has been previously stated, S-CO_2 is the main choice for this future power plant, the European confidence for the technological readiness comes from the good achievements on the S-CO_2 matter and their brilliant future perspectives.

For further reading into the story of S-CO_2 and its current stage, the reader is strongly recommended to look into the PhD thesis of Dostal [44] and Crespi's paper [49].

4 Electric efficiency assessment for DEMO1 and DEMO2 scenarios

In this chapter a series of layouts for a pulsed, DEMO1, and a steady-state scenario, DEMO2, are proposed. For DEMO1, the model used for the thermal energy storage is also introduced. A sensitivity analysis will be done for these layouts. An optimization process with the electric efficiency of the power plant as the figure of merit will be the basis for the comparison between layouts.

Two types of DEMO-like reactors are going to be used as the heat source of the fusion power plants. Firstly, the DEMO Baseline 2018 will be used as the current established design (DEMO1) followed by a more advanced steady-state machine (DEMO2) where some of the constraints shown in the Baseline are eliminated and higher temperatures can be achieved through all the machine. For the DEMO1 scenario, three layouts have been proposed each one with three modifications, adding up to nine layouts. Meanwhile, for DEMO2 two designs will be studied.

For each layout, its boundary conditions and their effects on the layout will be explained. An optimization process with the electric efficiency as the figure of merit will be used to compare the proposed layouts. The temperature and pressure at the turbine and compressor inlets together with the mass fraction flowing through the secondary compressor will be varied to achieve said maximum on the electric efficiency. As the working fluid is carbon dioxide, within a S-CO_2 cycle, a pinch point analysis will be carried out whenever a heat exchanger comes close to the critical point, the reason after this was explained in chapter 3.

For these simulations the *EES* (Engineering Equation Solver) software is used [50]. EES is a numeric solver developed by F-Chart that can solve up to 6000 coupled non-linear equations in its commercial version. EES features a vast library of thermodynamic properties of fluids, in which CO_2 is contained. Its ease of use is one of its strengths as the equations can be written with no strict order or structure. The software is able to subdivide the introduced equations in blocks of interrelated equations that can be solved separately.

Two different fluids can be found in EES thermal-fluids library related to carbondioxide:

CO2 and CARBONDIOXIDE. The first assumes it is an ideal gas meanwhile the second is a real gas modeled by the fundamental equation of state of Span and Wagner [51] which is defined up to 1100 K and 800 MPa. For this work the real gas fluid (CARBONDIOXIDE) will be used. The reference value for enthalpy and entropy is defined as zero in standard conditions (25ºC and 1 atm).

4.1 Pulsed layouts

These models will follow the DEMO Baseline 2018. As it was stated in chapter 2.4, the DEMO 2018 Baseline proposes a breeding blanket Model B (HCPB). In this section, the boundary conditions to which all following layouts will be subjected are enumerated and explained.

- **Maximum temperature in divertor and shield:** DEMO Baseline 2018 works with a water-cooled divertor and shield. T_{max} = 150ºC.
- **Maximum temperature in secondary cycle:** limit imposed by the structural material used in the HCPB model. EUROFER 97 cannot withstand more than 550ºC. A safety buffer has been applied, bringing the maximum achievable temperature of the secondary cycle at 500ºC.
- **Maximum pressure in secondary cycle:** this maximum is based on the ordinary maximum pressure in S-CO_2 power plant designs. p_{max} = 280 bar [17], [52].
- **Minimum pressure in secondary cycle:** the minimum pressure must be above the critical pressure that is at 73.77 bar and 30.98ºC, a safety buffer is included to dismiss safety problems. p_{min} = 75 bar, for this pressure T_{min} = 36ºC.
- **Equipment efficiencies:** [52] and [53] suggest an efficiency of 88% for compressors and 93% for turbines.

Current gas turbines and turbomachinery power plants are not prepared to work efficiently in a pulsed manner. On one hand, gas turbines have low efficiencies at reduced loads, the loading/unloading ramps will be at low efficiencies. Besides cyclic operation affects to the residual life of gas turbines drastically due to the linked mechanical stresses. This already happens in commercial combined cycles with frequent start and stop operation. This is not a new problem, a cyclic operation is a common problem faced by the thermosolar power industry and has been normally solved by adding thermal energy storage (TES) to the equation.

TES function is to accumulate thermal energy during the discharge time, to gradually release it during the time between pulses (known in the DEMO Baseline 2018 as dwell time). Pulse and dwell times are taken form the DEMO Baseline 2018, being 120 and 30 minutes respectively. The power distribution during pulse ensure that the same power (before TES efficiency) arrives at the power cycle at any given time, this is 80% of the power goes to the power cycle and the remaining 20% heats up the TES system. For subsections

4.1.1, 4.1.2 and 4.1.3, cycle efficiency will be calculated as [53]:

$$\eta_{cycle} = \frac{\dot{W}_{elec}}{\dot{Q}_{DEMO} * \frac{t_{pulse}}{t_{pulse}+t_{dwell}}} = \frac{\dot{W}_{elec}}{\dot{Q}_{DEMO}} * 1.25 \tag{4.1}$$

With W_{elec} being the electric power generated from the turbine after powering the turbines and Q_{DEMO}, the total thermal power coming from blanket and first wall, divertor and shield. W_{elec} is calculated during pulse time, this is as a steady state cycle that is fed 80% of Q_{DEMO}.

Section 4.1.4, will take the most promising layout and take a more accurate approach on the thermal storage system impact on the efficiency.

4.1.1 Layout A

This cycle features a regenerator in two steps, called HTR (High Temperature Regenerator) and LTR (Low Temperature Regenerator) and an intermedium compression where a fraction of the mass flow, α, bypasses the cooler. The rest of the mass flow passes the cooler, the main compressor and starts heating up due to the heat coming from the divertor, the shield and the LTR. In this step, both mass fluxes rejoin and achieve its peak temperature after the contribution of the HTR and the blanket. At this point, it can enter the turbine again and restart the cycle. This layout is represented in figure 4.1

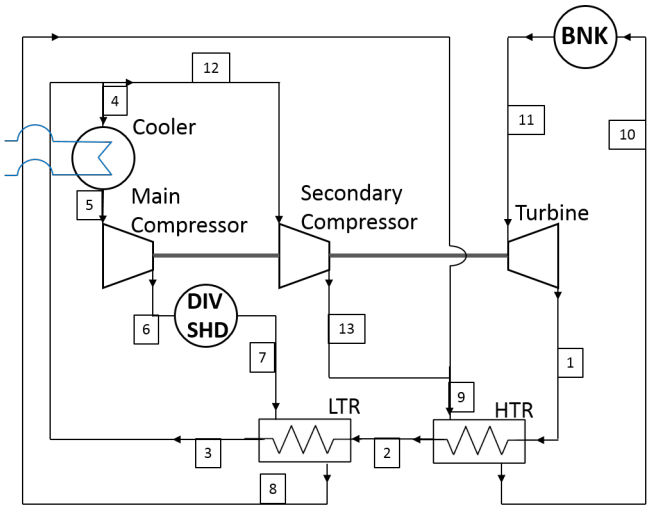

Figure 4.1 Layout A. With both regenerators in the low pressure side before the secondary compression.

In the high temperature regenerator, the pinch temperature (the minimum temperature difference at the heat exchanger, the issues of the pinch point in S-CO_2 were introduced in chapter 3) will be set at 4ºC [54], [55]; meanwhile in the low temperature regenerator

it will be of 4.5ºC to account the change of the variation of the thermal properties of the supercritial carbondioxide near its critical point. Those values will be used by default if not violation of these limits occur inside the heat exchanger (with special attention to LTR). Otherwise, this values will be increased.

As all layouts following the DEMO Baseline 2018, temperature achievable through passing by the divertor and shield cannot surpass 150ºC. The fraction of mass flow that is compressed by the secondary compressor is one of the optimization variables but it must fulfill that the LTR pinch point does not become too low. The other optimization variables are the inlet temperatures and pressures to the turbine and to the main compressor. Those are expected to be the maximum possible for the turbine and the minimum for the compressor as this achieves the highest enthalpy jump in the turbine and, therefore, the largest electricity production possible.

Layout A.1 (represented in figure 4.2) is the same cycle as in layout A, but the positioning of the LTR differs. Now the LTR is exactly after the main compressor, this means that the hot flow in the LTR can get to a lower temperature thus getting a lower wasted heat in the cooler. However, the restriction of 150ºC outside the divertor and shield must be taken into account, this will severely restrict the mass fraction, α, that can bypass the main compressor.

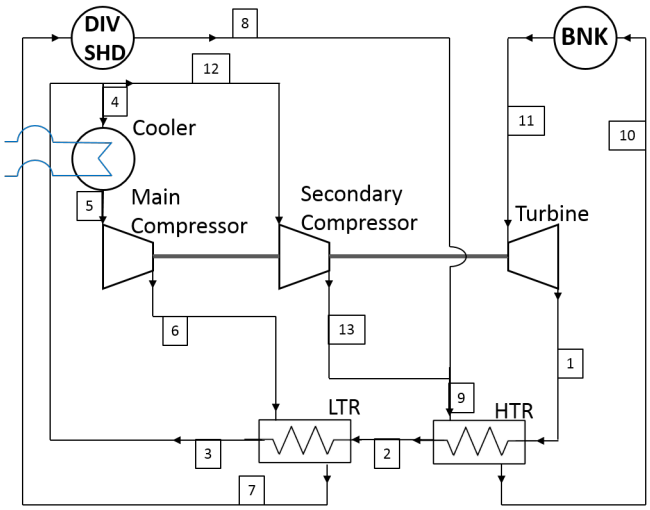

Figure 4.2 Layout A.1. With both regenerators in the low pressure side before the secondary compression and LTR before divertor and shield.

Layout A.2 (figure 4.3) cuts the heat input coming from the divertor and shield. Avoiding the temperature restriction coming from using those two heat sources. However, discarding divertor and shield is expected to tax the efficiency of the system, which effect is dominant will determine the suitability of this specific layout.

A sensitivity analysis has been performed for all thee layouts, modifying the temperature and pressure at the turbine inlet, pressure at the main compressor inlet and the mass fraction that goes through the secondary compressor (α). For the pressure in the main compressor a

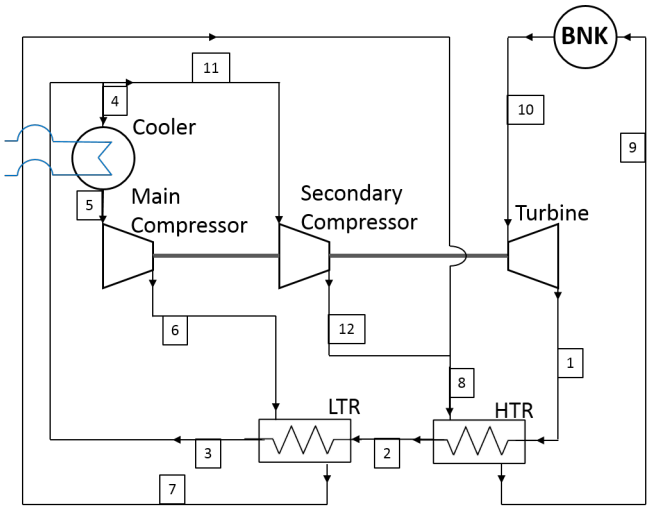

Figure 4.3 Layout A.2. With both regenerators in the low pressure side before the secondary compression and no heat coming from divertor and shield.

temperature of 30ºC has been set if the pressure is above 80 bar, on the contrary, if it is below 80 bar, temperature grows lineally from 30ºC to 36ºC at 75 bar. This difference in the input temperature avoids crossing the critical point (73.77 bar and 30.98ºC) and will be used for layouts A to C and its modifications.

Figure 4.4 shows the sensitivity analysis for the turbine inlet parameters. For both parameters, temperature and pressure, the maximum possible result to be the optimum values. For the temperature, the growth trend is equal for all layouts type A. But in the pressure analysis layout A.1 appears as the one most benefited for this increase, while A.2 efficiency stays rather constant above 240 bar.

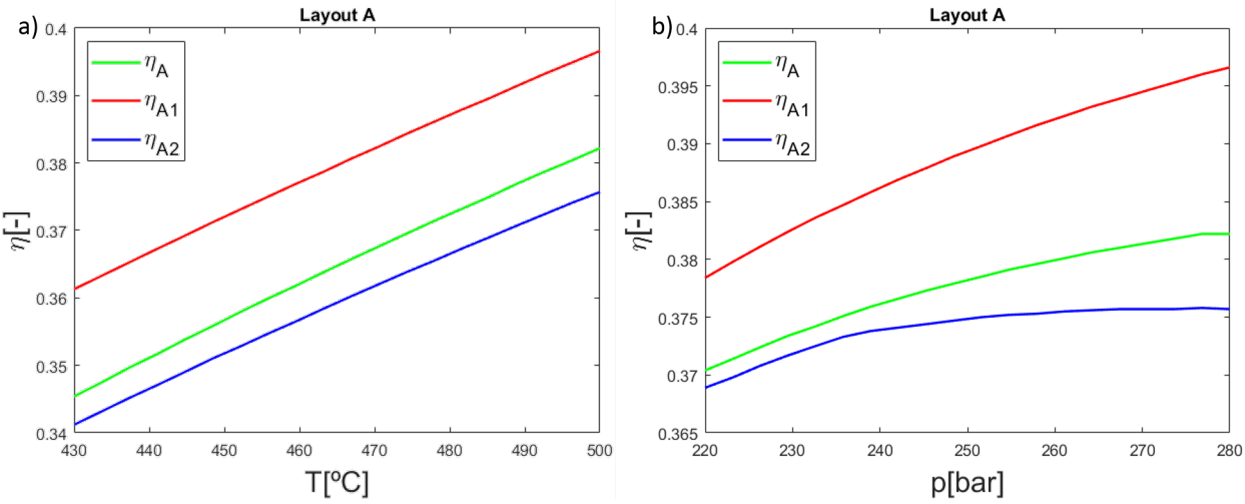

Figure 4.4 Sensitivity analysis for layouts type A. Varying temperature and pressure at the turbine inlet .

The mass fraction presents a maximum around 0.3-0.35. This maximum is not achieved

in layout A.1 as the temperature in the shield would exceed the limit of 150ºC for an α greater than 0.08. The effect of reducing the minimum pressure of the system has little impact until 78 bar are reached, when a drastic decrease on the efficiency is denoted partially. This is due to the increasing temperature (pressure is below 80 bar) and because of the varying properties near the critical point. Layout A is the only one with a slight benefit on decreasing its pressure, reaching its maximum at 79 bar.

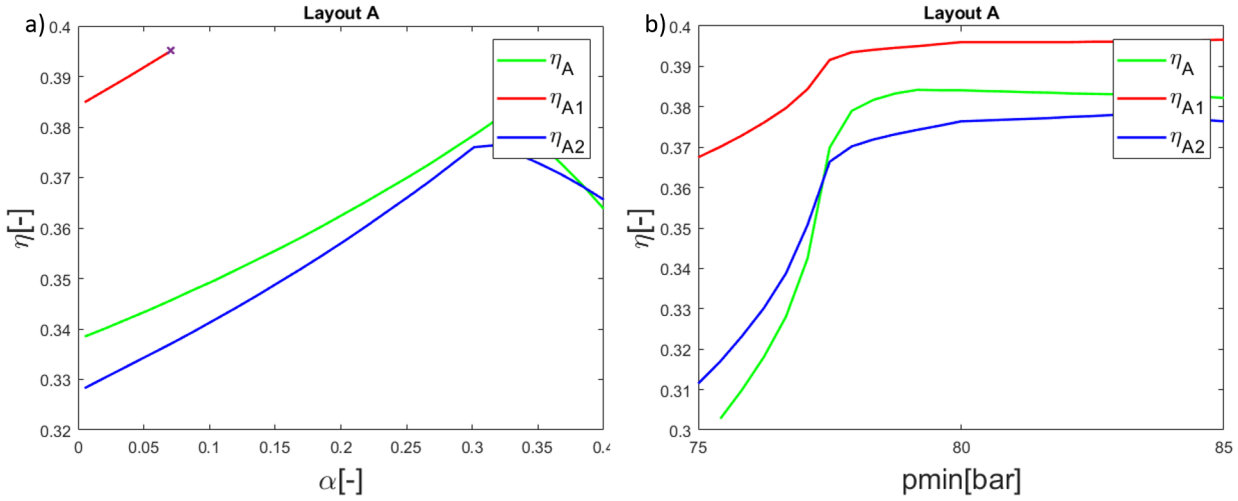

Figure 4.5 Sensitivity analysis for layouts type A. Varying mass fraction (α) and pressure at the compressor inlet.

On all sensitivity analysis layout A.1 has come consistently on top. Maximum efficiency has been achieved for p_5 = 85 bar, T_{12} = 500ºC, p_{12} = 280 bar and α = 0.08; getting an efficiency of 0.3951. In this maximum, the T-Q analysis of both regenerators have resulted in a positive solution with no violations of the pinch temperature limit inside the heat exchangers. Figure 4.6 represents this T-Q analysis for the LTR of layout A.1.

4.1.2 Layout B

Type B layouts explore the possibility of not using an intermediate compression, this removes the power consumption of the secondary compressor at the cost of evacuating more power at the cooler as bigger mass flow through this equipment.

The first layout, represented in figure 4.7, has only one regenerator. The regenerator is after the divertor and shield (equivalently to layout A.1), but, as there is no secondary compressor, the LTR would be following HTR so therefore only one regenerator is needed.

Layout B.1 recovers a structure with two regenerators as the LTR is situated before divertor and shield. This design is equivalent to layout A.1 but with no secondary compressor. This design has the flaw that the LTR has to provide an outlet temperature at the high pressure side substantially lower than 150ºC as the temperature outside the shield is capped at 150ºC. The layout is represented in figure 4.8.

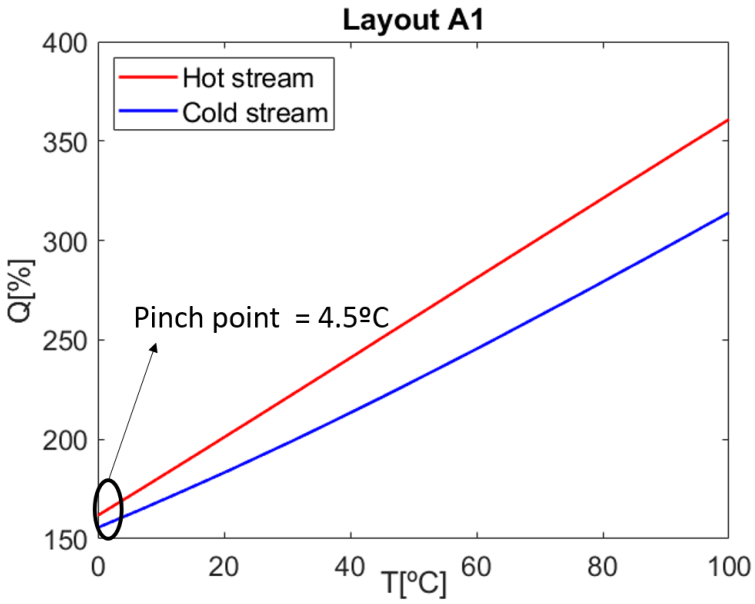

Figure 4.6 T-Q diagram of the LTR of layout A.1. The pinch point is found at the low temperature inlet to the heat exchanger.

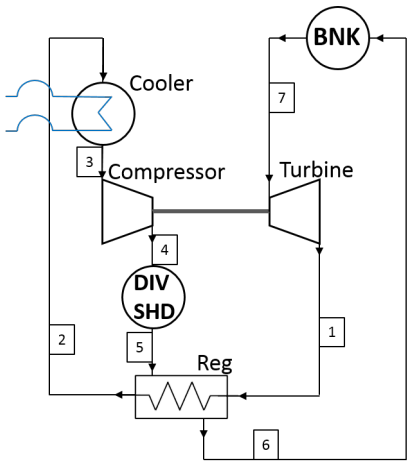

Figure 4.7 Layout B. With single regenerator.

Layout B.2 (figure 4.9) is the less equipment intensive of all layouts as the secondary compressor, divertor HX and shield HX are retired from the layout converting it into the simplest possible version. As there isn't divertor or shield heat exchangers, both regenerators are condensed into a single one.

The sensitivity analysis of these layouts will vary the inlet pressure and temperature for the turbine and the inlet pressure for the compressor. Again, for the pressure at the compressor the temperature will rise if pressure goes below 80 bar.

The sensitivity analysis graphed at figure 4.10 show that to increase the efficiency, temperature and pressure must be as high as possible. These results are coherent with layouts type A as more temperature and pressure means a larger enthalpy jump at the turbine.

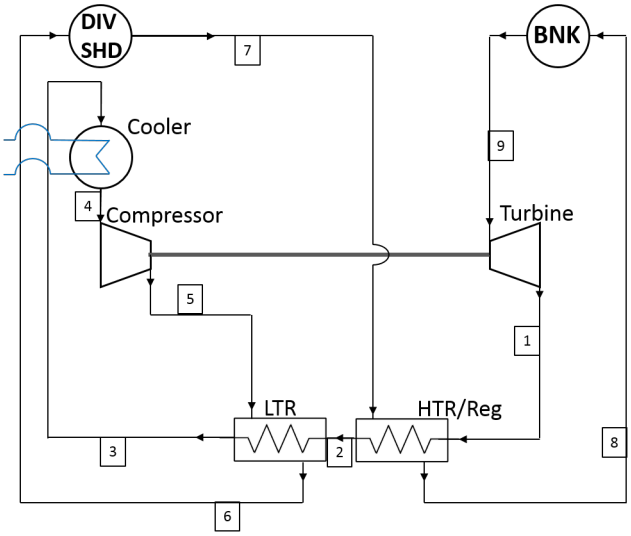

Figure 4.8 Layout B.1. With LTR before divertor and shield and HTR after them.

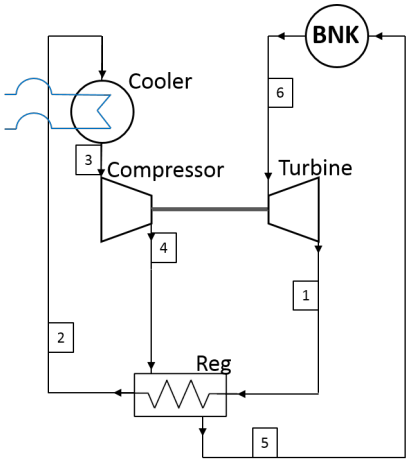

Figure 4.9 Layout B.2. With single regenerator and no heat coming from divertor and shield.

Figure 4.11 shows how the efficiency of the plant changes with the pressure at the compressor intake. Layouts B and B.2 follow the general trend of a maximum around 80 bar, but this trend isn't followed by layout B.1 which efficiency keeps on growing despite the turbine jump is decreasing. Although this may seem contradictory at first, the loss of efficiency due to a smaller enthalpy difference in the turbine is compensated by the extra power saved in the regenerator.

As this trend drags the minimum pressure of layout B.1 far from the critical point, following a supercritical CO_2 cycle does not make sense anymore. And, therefore, a Brayton cycle could be an interesting option for this layout as it will not be forced to work at supercritical pressures and a larger efficiency could be obtained.

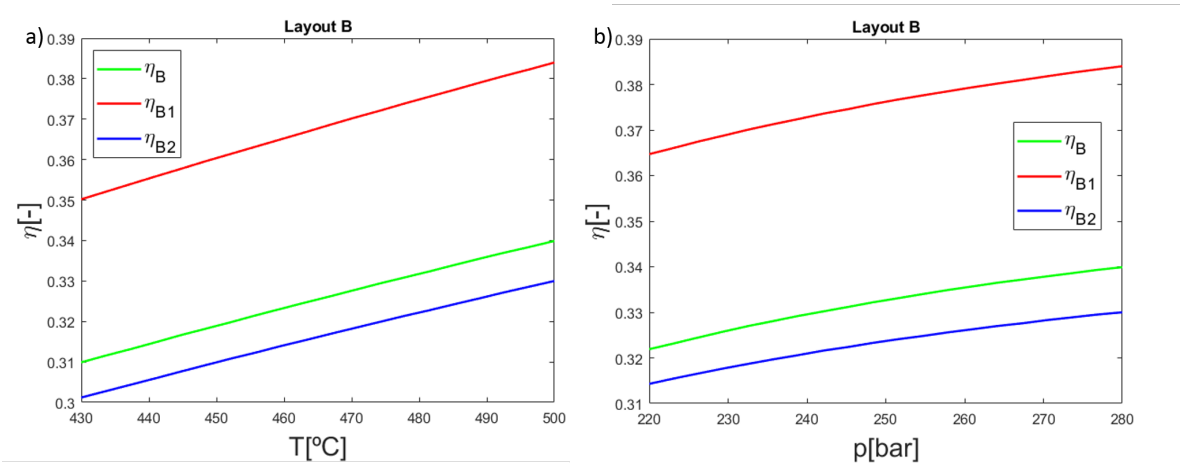

Figure 4.10 Sensitivity analysis for layouts type B. Varying temperature and pressure at the turbine inlet.

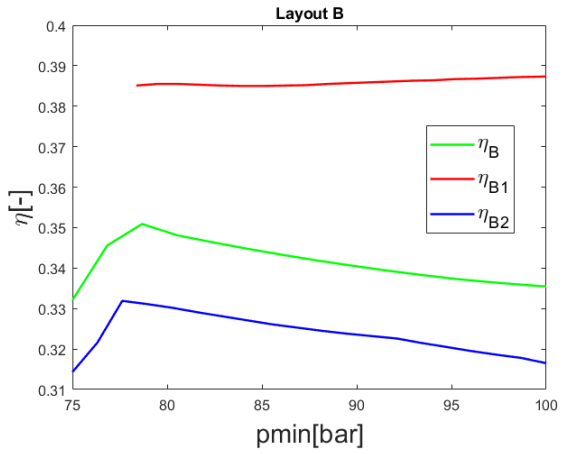

Figure 4.11 Sensitivity analysis for layouts type B. Varying pressure at the compressor inlet.

4.1.3 Layout C

This type of layout gets back the secondary compression, but now it is placed between both regenerators in its hot side. This means that now the low temperature regenerator will have the same mass flow at both sides and, therefore, α can't be used any longer to strongly modify the outlet temperature at the high pressure side.

As in the other two layout typologies already shown, layout C is characterized by the LTR regenerator in the high pressure side being situated after divertor and shield. This layout is represented in figure 4.12.

Layout C.1 (in figure 4.13) inverts the positioning of LTR in the high pressures side with divertor and shield. Thus letting LTR in the low pressure side to get to lower temperatures and, therefore, increasing the efficiency of the heat exchanger. But the temperature limit settled by the DEMO 2018 Baseline will cap the temperature achievable at divertor and shield and, by extension, at the LTR in the high pressure side.

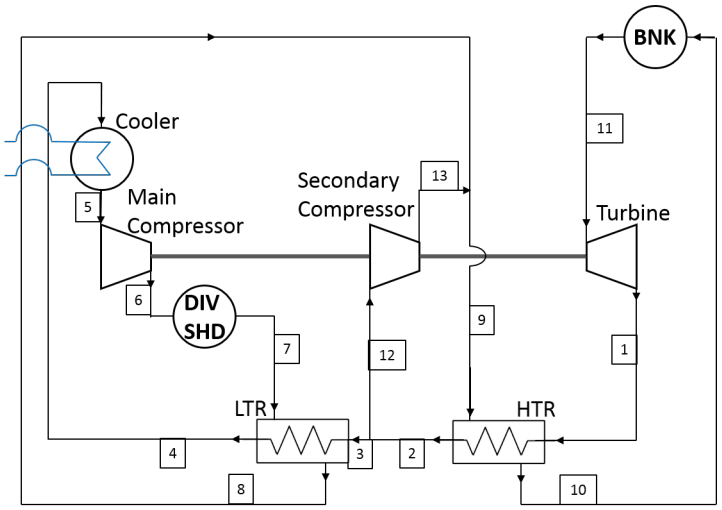

Figure 4.12 Layout C. With the secondary compression dividing both regenerators in the low pressure side.

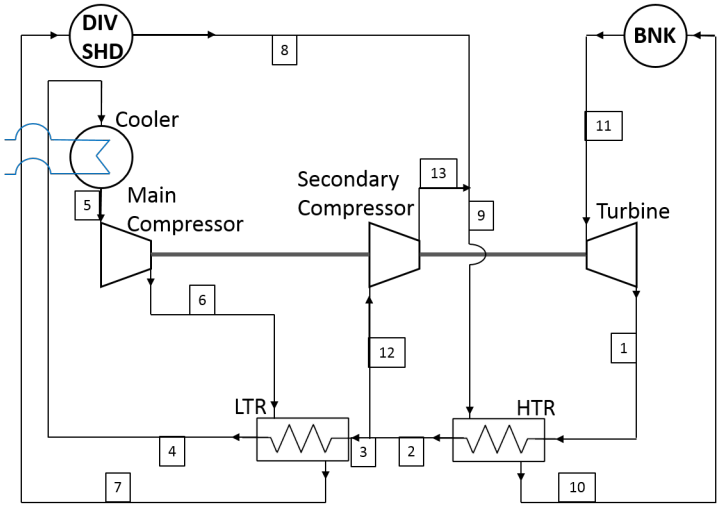

Figure 4.13 Layout C.1. With LTR before divertor and shield and HTR after them.

The last of the type C layouts is C.2, shown at figure 4.14. It does not use the power coming from divertor and shield to eliminate the limitation on temperature they imply, at the cost of less available heat power.

The sensitivity analysis that have been done for these layouts are the same than in the type A case. This is pressure and temperature at the turbine inlet, pressure at the compressor inlet and mass fraction (α) going through the secondary compression.

Figure 4.15 starts with the intake parameters for the turbine. As in the other six studied cases the cycle tries to get the maximum possible temperature and pressure to ensure the largest power production possible at the turbine.

Lastly, α and p_{min} analysis are plotted on figure 4.16. For layouts C and C.2 efficiency slowly increases with α until peaking around 0.2-0.3, just to collapse rapidly after this point. Layout C.2 does not get to reach this maximum as the temperature limit on divertor

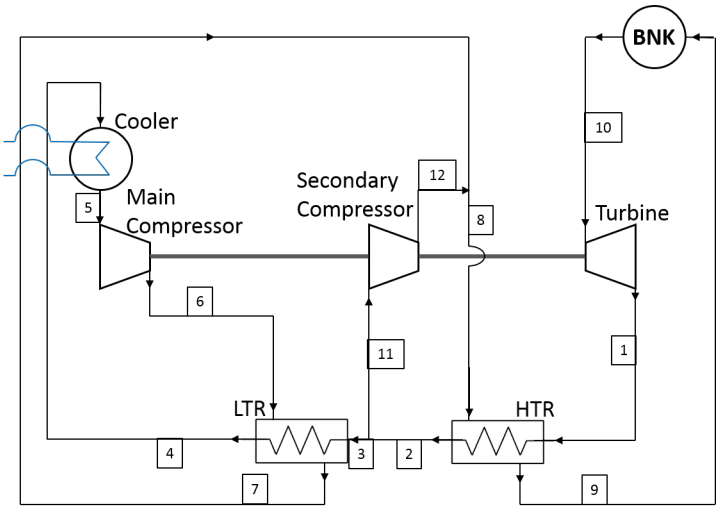

Figure 4.14 Layout C.2. With both regenerators separated by the secondary compression and no heat coming from divertor and shield.

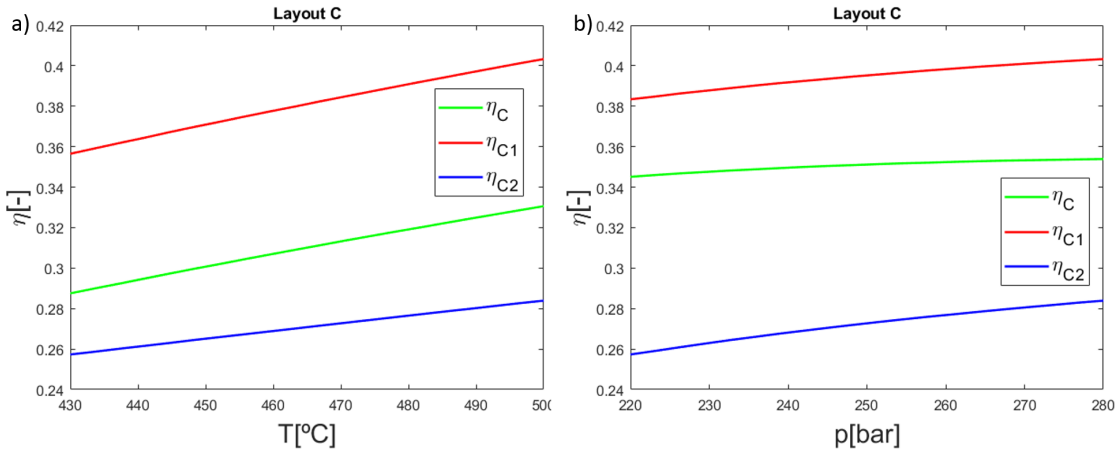

Figure 4.15 Sensitivity analysis for layouts type C. Varying temperature and pressure at the turbine inlet..

and shield would be surpassed. p_{min} variation shows that the maximum is achieved for all layouts for a similar pressure (between 77-79 bar) and after this point the efficiency is rather constant.

Through all nine presented layouts types X.1 (with X being A, B, C) have come consistently on top in terms of efficiency. The maximum efficiency for these "winning " cases are shown in table 4.1. Of these layouts, layout B.1 presents a series of parameters that suggest modeling it after a Brayton cycle instead of a supercritical one. Layout A.1 stands as the one with the highest possible efficiency, due to this a more precise version of this layout will be studied in the section 4.1.4 and this layout will serve as the base for layouts of type D in section 4.2.

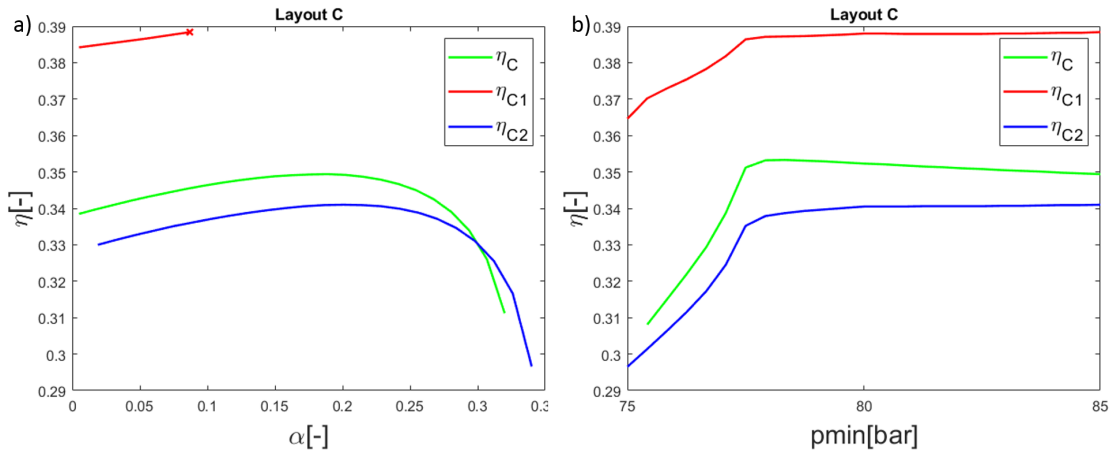

Figure 4.16 Sensitivity analysis for layouts type C. Varying mass fraction α and pressure at the compressor inlet.

Table 4.1 Sensitivity analysis for layouts type C. Varying mass fraction α and pressure at the compressor inlet.

	η [-]
Layout A.1	0.3966
Layout B.1	0.3908
Layout C.1	0.3884

4.1.4 Layouts with Thermal Energy Storage Model

In this section a more precise model of the thermal energy storage (TES) is proposed to get a more accurate estimation of the efficiency of a real fusion power plant working in pulsed state. As previously stated, pulse time will be 120 minutes and dwell time, 30 minutes; following the estimations of the DEMO Baseline 2018. The transition time between one state and the other, ramp time, is going to be taken as a free parameter that will be analyzed parametrically. A complete cycle will always last 150 minutes, this means that ramp time is directly taxing how long is the pulse and dwell time. For instance, figure 4.17 uses tramp = 10 min which means the power plant will only be working at full power during 110 minutes and powered by the TES for 20 minutes.

In figure 4.17 a complete cycle of the power supplied to the sCO2 cycle against time is shown. During the pulse time 80% of Q_{DEMO} is transferred, while, during dwell time, the TES system start to provide power, but some of it is destroyed as heat losses to the environment. TES efficiency is defined as the fraction of the received power from the reactor that is given to the power cycle (equation 4.2). As the energy is kept as heat during the whole storage process, the system can achieve really high efficiencies. Some authors [53] just suppose a 100% efficiency for a first approximation like the studied here; [56] in relation to a TES for a solar thermal power plant proposes an efficiency range between 93-97%. For this specific case, a 95% efficiency was chosen, nonetheless the effect of the

TES thermal-to-thermal efficiency will be studied for a certain range.

$$\eta_{TES} = \frac{Q_{TES \rightarrow cycle}}{Q_{DEMO \rightarrow TES}} \tag{4.2}$$

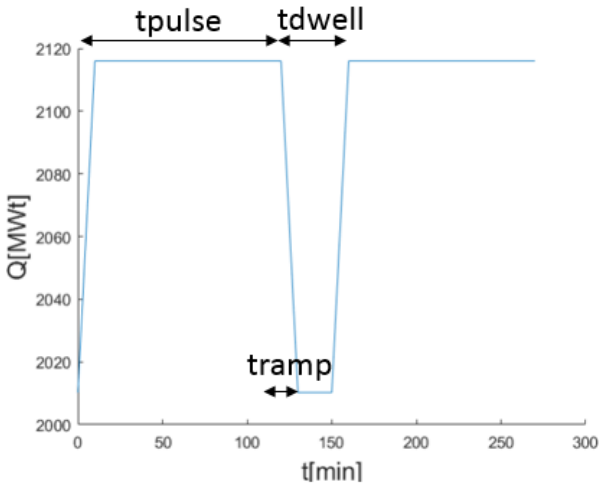

Figure 4.17 $Q_{toCycle}$-time cycle of a pulsed-state fusion power plant. Pulse and dwell time follow the DEMO 2018 Baseline and ramp time has been set to 10 minutes.

As the working conditions change while the power plant is being fed by the storage system, the efficiency of the turbomachines is expected to decrease from one point to the other. A 2% decrease for the turbine and 3% for the compressor have been assigned. The compressor impact is more significant as these machines are more sensitive to changes in their work point than turbines. In summary, efficiency during pulse time will be of 93% and 88% (values taken from [52] and [53]) for turbine and compressor respectively and for the dwell time will be down to 91% and 85%.

Electric efficiency of the power plant will be calculated in terms of energy instead of power like has been calculated in previous cases. The energy produced during the ramp will be calculated as if the power production changed linearly during one stage to the other, therefore this energy will be just the area under that triangle. Mathematically, the electric efficiency of the power plant is calculated as follows in equation 4.3.

$$\eta_{cycle} = \frac{W_{elec}}{Q_{DEMO}} = \frac{\dot{W}_{pulse} * (t_{pulse} - t_{ramp}) + \dot{W}_{dwell} * (t_{dwell} - t_{ramp}) + W_{ramp}}{\dot{Q}_{DEMO}} \tag{4.3}$$

With W_{elec} being the electric energy produced during a complete cycle; Q_{DEMO}, the energy produced by DEMO during a complete cycle; $\dot{W}_{pulse}$, electric power produced during pulse time; $\dot{W}_{dwell}$, electric power produced during dwell time and W_{ramp}, the electric energy produced during ramp time.

The effects of the application of this model will be shown for layout A.1 as it stood up as the most promising one in terms of efficiency in the previous comparisons. The rest of cases will be summarized at the end of this section.

A parametric analysis of the layout has been made studying the same parameters that were studied for layout A.1, this is pressure and temperature at the turbine inlet, pressure before compressor and α. But two cases must be analyzed now, one during pulse time and the other during dwell time. From the pulse stage to the other the mass flow is kept constant, this means that during dwell time the temperature at the turbine entry is not a parameter anymore and is fixed by the cycle. The intention is to keep the working conditions from one mode to the other as similar as possible to prevent the equipment worn out. To accomplish this, the maximum temperatures in the heat exchangers receiving the power of the tokamak have been kept the same: maximum temperature at blanket and first wall of 500ºC and maximum temperature at divertor and shield of 150ºC.

The first set of parameters to study, the inlet parameters to the turbine, are shown in figure 4.18. Parameters referred to the dwell period are marked with a subindex p. In the first part of the figure only the temperature during pulse time is modified as it was already explained before. The temperature during the dwell time is plotted as well to show that due to a lower heat power reception and the same mass flow, maximum temperature cannot be as high as during the pulse time.

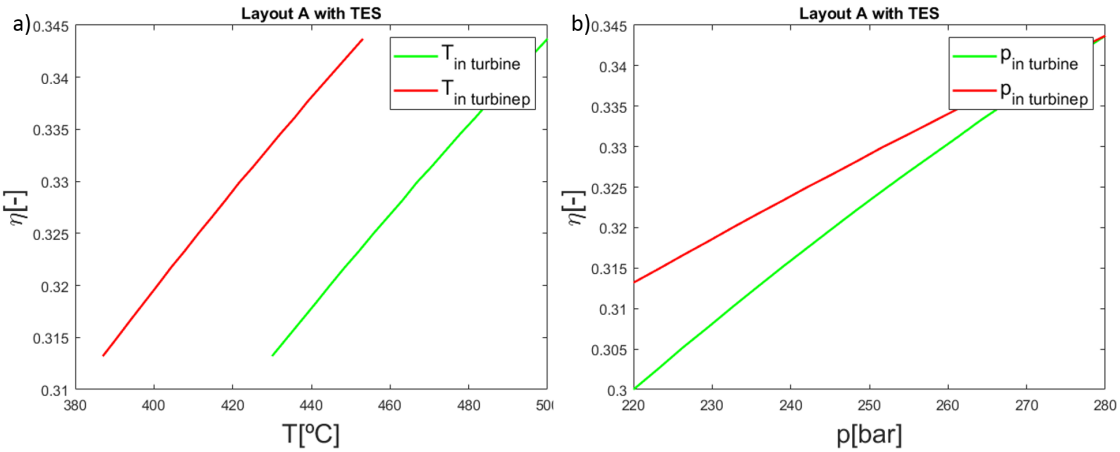

Figure 4.18 Sensitivity analysis for layouts type A.1 with Thermal Energy Storage. Varying temperature and pressure at the turbine inlet.

As usual, the most efficient situation results in the highest possible temperature and pressure at the turbine inlet. They are limited by the 500ºC limit imposed by the EUROFER steel and by the pressure conventions to avoid excessive sizing in the piping and in the equipment.

The sensitivity analysis of this layout continues with figure 4.19, where the mass fraction α going through the secondary compression process and the pressure at the main compressor inlet are varied. Both figures are cut abruptly, for larger values the limit on divertor and

shield temperatures is violated. In this figure a trend that was slightly visible at figure 4.18 appears severely strong, varying the parameters related to dwell time barely modifies the electric efficiency of the whole power cycle. Not only the power produced during pulse time is larger but it is also for a significant longer time, therefore the approximation of similar parameters during pulse and dwell time protects the machinery and do not fall into noticeable differences from a mathematical optimum. This lack of importance is increased with longer ramp times.

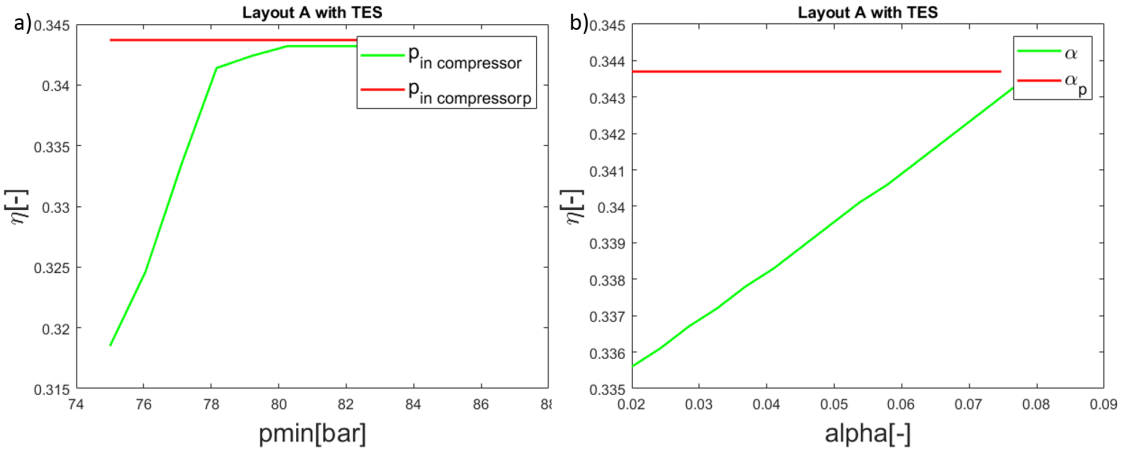

Figure 4.19 Sensitivity analysis for layouts type A.1 with Thermal Energy Storage. Varying mass fraction α and pressure at the compressor inlet.

The influence of varying the ramp time can be easily seen from equation 4.3. Due to the simplicity of this first approximation model, the response of the system to a changing ramp time appears to be linear and this is refuted by figure 4.20. In a future model, with a more realistic approach the transition between one state to the other will be smoothed to take into account the thermal inertia of all components. It is no surprise that shorter ramp times mean better efficiencies as this means that the cycle is working longer at nominal power. DEMO 2018 Baseline estimates a ramp time of 500 seconds as marked in figure 4.20.

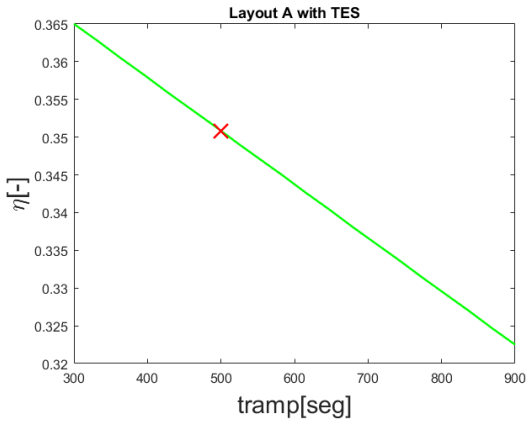

Figure 4.20 Sensitivity analysis for layouts type A.1 with Thermal Energy Storage. Varying ramp time.

Comparing this TES model with the simplified one used for the previous layouts show that this is a more conservative and precise one. For this layout, optimum efficiency has passed from 0.397 to 0.344, a large change that servers as an example of the importance of refining the TES model. However, the goal of the first analysis carried on layouts type A, B and C was not to get an accurate grasp of the efficiency of each layout, but to order them in relative importance and to get a sense of what can mean a supercritical carbon dioxide powered by a DEMO-like fusion plant. The results for all studied layouts are summarized in table 4.2.

Table 4.2 Comparison between the simplified model and the TES model.

	Simplified model	**TES model**
Layout A	0.384	0.333
Layout A.1	0.397	0.344
Layout A.2	0.376	0.326
Layout B	0.334	0.290
Layout B.1	0.334	0.290
Layout B.2	0.386	0.334
Layout C	0.354	0.307
Layout C.1	0.88	0.337
Layout C.2	0.341	0.296

4.2 Steady-state layouts

In this section a steady-state layout is presented based on layout A.1 due to this being the most promising layout of the cases studied in the past section, this new layout will be named layout D. Schematically, layout D (figure 4.21) is identical to layout A.1, the difference lies in an less restrictive set of limitations over the cycle parameters. This section aims to model a more advanced power cycle for a more optimistic DEMO were higher temperatures can be achieved and conditions are more favorable for power production.

One of the key problems of layout A.1 was the low mass flow fraction that flowed through the secondary compressor, this was due to the temperature limitation that the DEMO Baseline 2018 imposed over heat coming from divertor and shield, now this limitation is removed so α is expected to increase until its maximum in efficiency is reached.

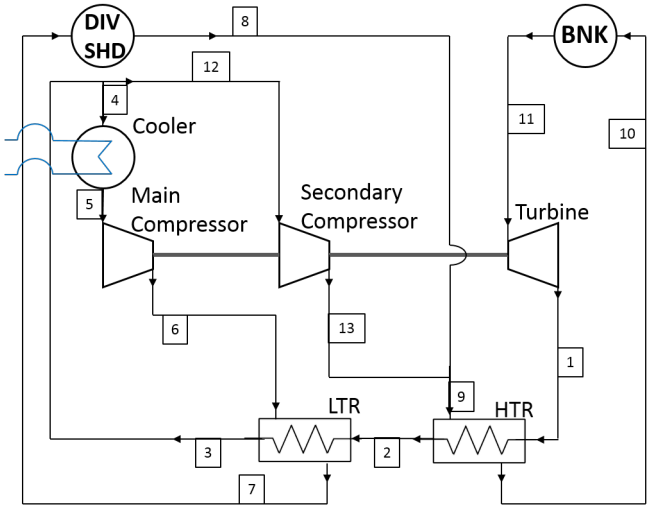

Figure 4.21 Layout D. With both regenerators in the low pressure side before the secondary compression and LTR before divertor and shield.

Restrictions on pressure are kept the same as they weren't set due to the DEMO Baseline 2018 but by the nature of a supercritical carbondioxide power cycle. Maximum temperature, on the other hand, can be increased as for this layout a better material is supposed to have replaced EUROFER 97 steel. CO_2 properties are calculated using Span and Wagner correlation (as it was explained at the beginning of this chapter), this correlation is validated until 1100 K; therefore the sensitivity analysis on the maximum temperature won't surpass the 800ºC mark. This is consistent with the applicability range of S-CO_2 cycles that don't aim to work at very high temperatures but in a medium to high range. For high range temperatures, a Brayton cycle is recommended as a more efficient and consolidated alternative.

A sensitivity analysis on the inlet parameters to the turbine (temperature and pressure) shows that, as in the rest of cases, the efficiency is positively affected by a hotter and more pressurized gas at the turbine entry (figure 4.22). A noticeable difference with the steady-state layout A.1 is the leap on the efficiency range, with an increase of 20 percentual points.

The effect of this change is not only the increased temperature, a wider range of possible α is also responsible as it is seen in figure 4.23. In its pulse-state equivalent, layout A.1, α was limited to 0.08 due to temperatures restriction on divertor and shield. Inlet pressure to the compressor presents its maximum around 80 bar as it has been previously seen in most layouts.

As it was expected, a steady-state layout which does not need TES, has laxer restriction

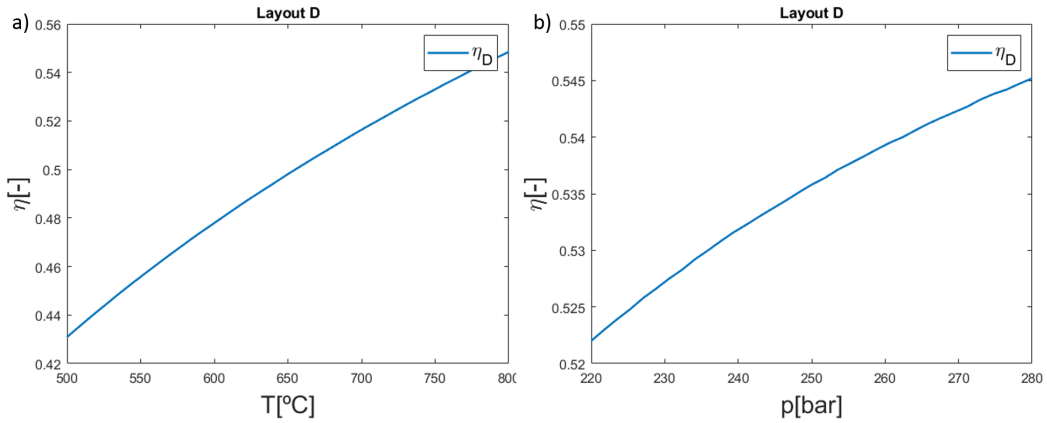

Figure 4.22 Sensitivity analysis for layout D. Varying temperature and pressure at the turbine inlet .

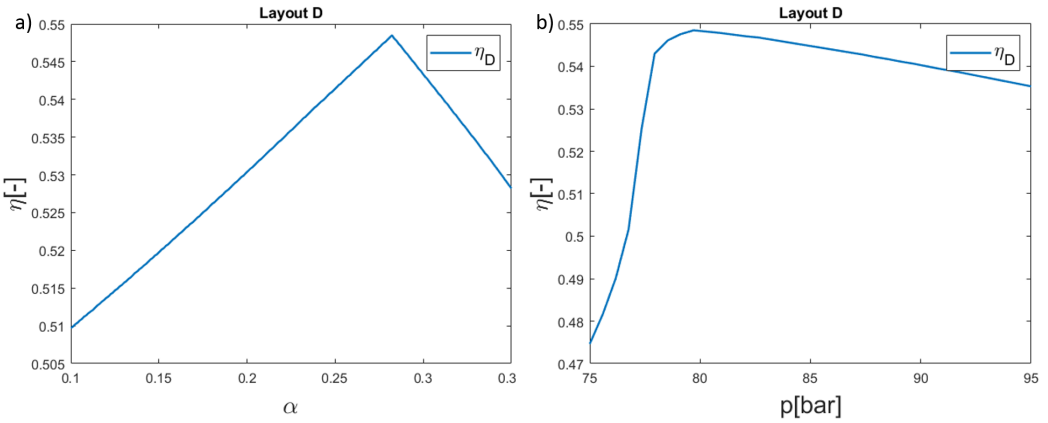

Figure 4.23 Sensitivity analysis for layout D. Varying mass fraction α and pressure at the compressor inlet.

on temperatures and is able to choose a wider range of α; provides more electric power with the same input heat power. To further increase this production, layout D.1 is proposed (figure 4.24). It features a second turbine with an intermediate heat exchanger from the blanket and first wall. So in this case, heat power coming from blanket and first wall is split into two heat exchangers, both of them placed just before entering into the turbine.

Two more parameters are added to the list already presented for layout D, inlet temperature and pressure for the second turbine (point 13 in figure 4.24). This pressure will dictate how the produced power is distributed between both turbines. High pressure at point 12 will mean little power in turbine 1 and the majority in turbine 2, the opposite would happen if the pressure were low. Despite p_{12} looking as a free parameter at first, theoretically the optimum pressure can be defined in equation 4.4 [57]:

$$p = \sqrt{\text{high pressure} * \text{low pressure}} = \sqrt{p_{11} * p_5} \tag{4.4}$$

To check this equation, a sweep on this parameter was done in figure 4.25. For said

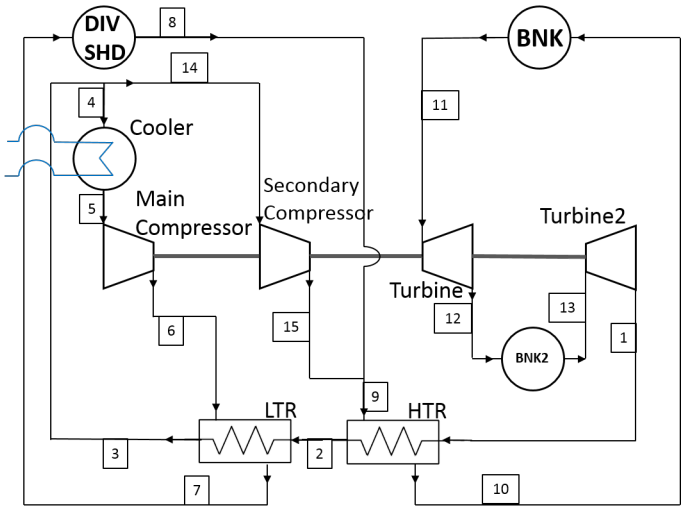

Figure 4.24 Layout D.1. Follows layout D but adds a second turbine with intermediate heat input fed by the blanket and first wall.

figure, p_{11} = 280 bar and p_5 = 79.21 bar; so optimum pressure is expected to be found at p_{12} = 148.9 bar. This is in fact what happens for the cycle under analysis, therefore p_{13} will not be a parameter anymore and it will be substituted by the value resulting from equation 4.4.

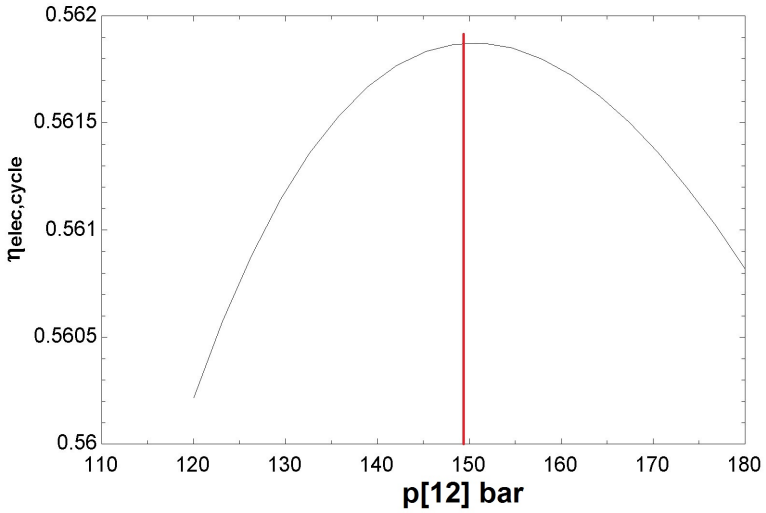

Figure 4.25 Pressure after first expansion vs. efficiency of the power plant. The maximum is obtained at the square root of the product of the maximum and minimum pressure at the cycle.

Sensitivity analysis starts with the temperature at both turbines intake and the pressure at the first one (figure 4.26). The first part of this figure shows the sensitivity due to temperature variation, those two temperatures are strongly linked as both are using the same heat source, $Q_{BLANKET}$. Therefore, not all temperatures are possible, this is visible

in the plot whenever a curve ends abruptly. This happens because the totality of the heat power has gone to one of the heat exchangers so it can grow any longer. As usual, the best working point occurs at the maximum of temperature (for both turbines) and pressure.

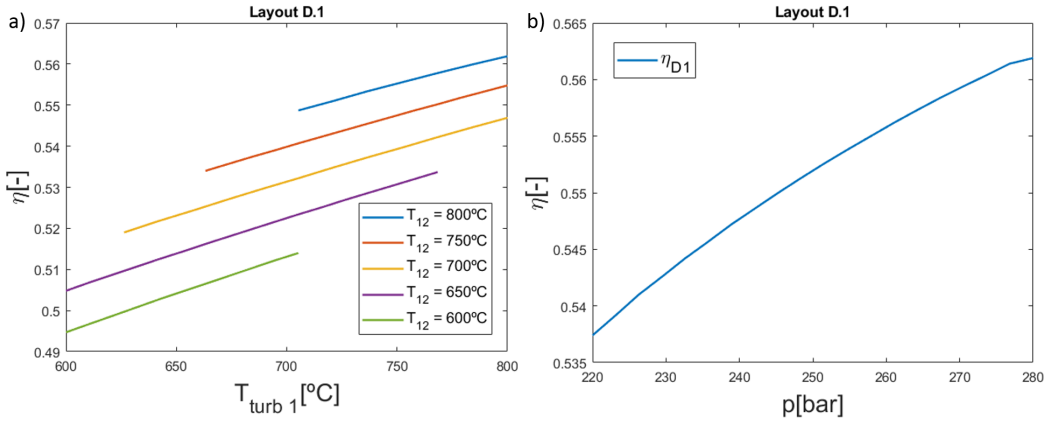

Figure 4.26 Sensitivity analysis for layouts type D.1. Varying temperature T_{12}, T_{14} and p_{14} .

The influence of α is shown in figure 4.27, the maximum is around 0.28. In this figure also inlet pressure to the compressor is represented, appearing the maximum at 79.71 bar.

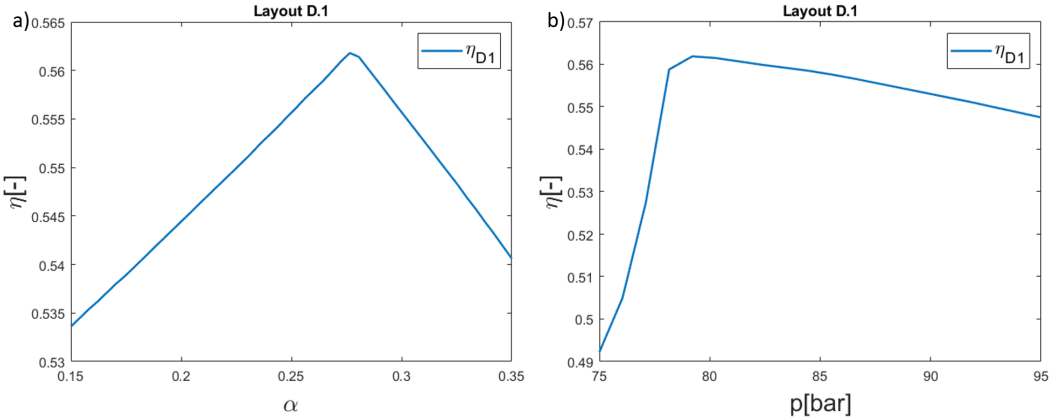

Figure 4.27 Sensitivity analysis for layout D. Varying mass fraction α and pressure at the compressor inlet.

Adding this second turbine has meant an increase in the peak efficiency of the cycle from 0.5484 to 0.5619. Said increase may seem small at first, but the true magnitude of the power produced and handled by the power plant must be taken into account. 36 MWe more are produced with the addition of the second turbine, a really noticeable difference that could mean the greenlight of a project of these circumstances.

Results for all simulations are summarize in table 4.3. The power plant efficiency takes into account the electric power consumption of the reactor.

Table 4.3 Overall plant optimized results for all studied layouts. Results for pulsed layouts follow the TES model.

	m [kg/s]	**W_{elec} [MWe]**	η_{cycle}	$\eta_{elec,\ plant}$
Layout A	8381	274.5	0.333	0.147
Layout A.1	7656	294.9	0.344	0.158
Layout A.2	7978	261.8	0.326	0.140
Layout B	7652	193.4	0.290	0.104
Layout B.1	7493	276.4	0.334	0.148
Layout B.2	6370	189.1	0.287	0.101
Layout C	7243	225.4	0.307	0.121
Layout C.1	7818	281.2	0.337	0.151
Layout C.2	7473	204.6	0.296	0.110
Layout D	8553	958.6	0.548	0.362
Layout D.1	8248	994.3	0.561	0.376

5 Economic estimations using PROCESS

Nine pulsed layouts for a DEMO1-like fusion power plant were studied in the previous section. For the steady-state, another two systems were analyzed, they showed better results as it was expected. PROCESS code is able to estimate the cost of a fusion power plant from the plasma physic and constructive parameters that define the reactor and using the thermal efficiency of the power cycle as an indication of how the power plant is built. Unfortunately, everything related to the power plant itself is just wrapped in the efficiency and the net electric output, it does not take into account the number of characteristics of the used equipment. Future work in these economic assessments will look for a more accurate approach regarding the power plant cost.

PROCESS defines thermal efficiency as the ratio of the produced electric power to the heat input. This is the efficiency that has been calculated for all layouts and was named as electric efficiency during the analysis shown in chapter 4.

Using the PROCESS code, the cost of four of the layouts is going to be estimated. For pulsed layouts, layout A.1 and its version with a refined model of the thermal energy storage; for steady-state, both available layouts, layout D and layout D.1. Inputs are the ones used to obtain the DEMO 2018 Baseline, the modified parameters are the related to the power plant itself, these are collected at table 5.1.

Table 5.1 Inputs directly associated to the power plant used for PROCESS. Rest of the inputs are at the end of each of the appendices.

	Layout A.1	**Layout A.1 TES**	**Layout D**	**Layout D.1**
DEMO type	pulsed	pulsed	steady-state	steady-state
$\eta_{\|\textbf{thermal}}$	0.3966	0.344	0.5484	0.5619
Net electric output [MW]	347.374	294.573	958.613	994.275

A summary of the estimations is exposed in table 5.2. In the appendices, the total

breakdown of costs is included together with all the plasma physics-related results that are out-of-the-scope of this work. The results included in this table are the ones judged to be the most representative ones. This table can be divided in three parts:

- Cost of some of the most characteristics systems, from power plant to power conditioning.
- Cost of electricity (COE)
- Simplified breakdwon of the final and total cost

Table 5.2 Associated costs for different layouts. For a complete breakdown, refer to the appendices.

	Layout A.1	**Layout A.1 TES**	**Layout D**	**Layout D.1**
Turbine plant equipment [M$]	156.58	151.06	210.85	215.15
Electric plant equipment [M$]	32.03	32.45	36.48	36.48
Heat rejection system [M$]	50.77	65.11	30.61	29.7
Vacuum systems [M$]	33.68	33.79	29.22	29.22
Power conditioning [M$]	145.36	145.10	173.86	173.86
Cost of electricity [$/MWh]	386.966	458.081	211.975	204.054
Fuel cost [m$/year]	639.80	649.11	713.66	715.2
Indirect cost [M$]	1173.91	1195.87	1364.90	1365.85
Plant direct cost [M$]	4183.58	4261.84	4864.21	4867.60
Total contingency [M$]	803.62	818.66	934.37	935.02
Constructed cost [M$]	6161.12	6276.37	7163.48	7168.46
Interest during construction [M$]	924.17	941.45	1074.52	1075.27
TOTAL CAPITAL INVESTMENT [M$	7085.28	7217.82	8238.00	8243.73

When talking about the viability of a power plant the three main metrics are observed: total investment, levelized cost of electricity and plant lifetime. Total investment for each layout is captured in table 5.2, that is the addition of the financial cost (interest during construction) and the cost of the construction itself. At the same time, the constructed cost is divided into direct and indirect cost, the direct cost contains a contingency budget that accounts for a 15% that is already added. In light of the results, total investment is not very dependent of the efficiency and net power output of the plant, not even a 2% increase in the pulsed layout comparison and less than 1% for the steady-state cases. The real increment comes from the DEMO technology, being the steady-state one billion dollars more expensive than the pulsed one.

The values obtained for the COE are in table 5.2, it is important to notice that the field name as fuel cost (following PROCESS output naming) contains the cost of replenishing divertor, blanket and other systems during the lifetime of the power plant. These components, specially the divertor, suffer the bombardment of highly energetic particles that will require its complete replacement once the damage is important enough. The cost of the

fuel itself has no real impact, accounting for only 0.2% of the COE; the biggest contributor is the capital investment with over a 70% of the total. Cost Of Electricity gives the price for what the energy must be sold in order to obtain zero benefit from a power plant. And it is in this parameter where the importance of an efficient power plant shines. There is a 200 $/MWh difference between the best (layout D.1) and worst (layout A.1 TES) scenarios. Layout A.1 TES, the most realistic scenario, doubles the COE of layout D.1. Therefore the importance of achieving the most optimal layout for the power plant to compensate the physics and engineering advancements supposed for layouts type D. Entler got to the same conclusion in his fusion energy economical analysis [22].

Making a comparison with current technologies is the next logical step, figure 5.1 shows this comparisson with renewable technologies for the years 2010 and 2016. Only the steady-state layouts are comparable, COE coming from studied pulsed design is so high that it gets out of limits for this figure. But layouts type D start with a better position. Actually, it competes with better prices than solar thermal in 2016. As this is a totally new technology it cannot be expected to enter and compete freely in the market without evolving through the learning curve. This figure illustrates the evolution of other renewable energies like photovoltaics that, despite starting with unsustainable high prices, have, nowadays, found its niche inside the electric grid. It is expected that a fusion power plant will follow a similar learning curve, being highly subsidized at the beginning and with the succession of newer generations (manufacturing costs can decrease down to 40% in the tenth generation [59]) , COE will go down enough to make it economically profitable by themselves.

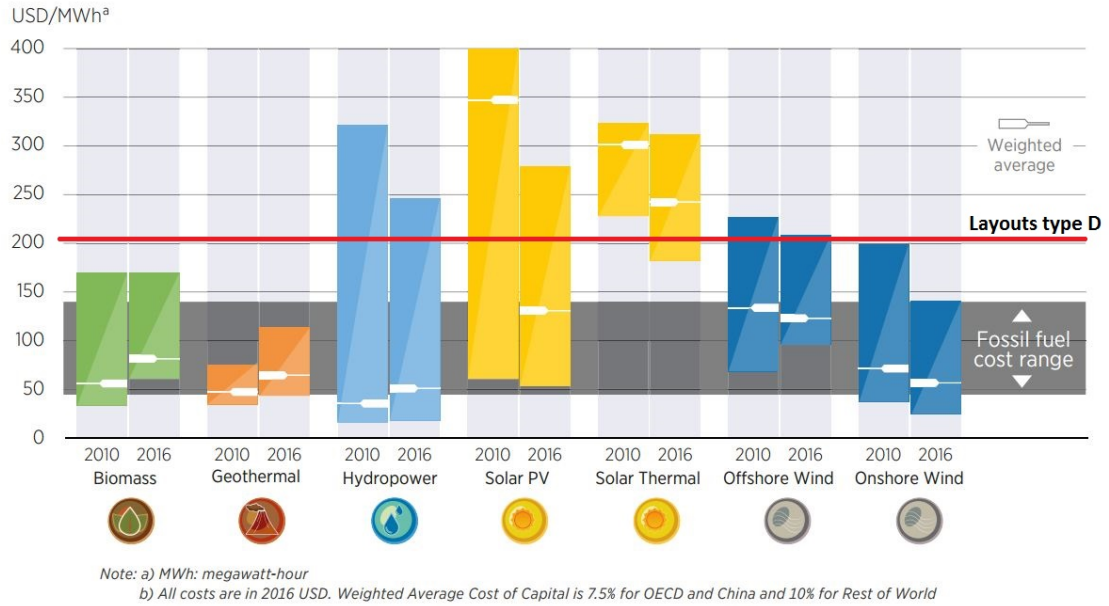

Figure 5.1 COE for different power sources for the years 2010 and 2016. COE of layouts type D is marked in red [58].

Finally, in table 5.3 the lifetime of the power plant and some of its components are shown, as well as the availability fraction. Blanket and divertor lifetimes are subjected to the damages received during its functioning. Plant lifetime, on the other hand, is in line

with fission reactors [60] and may be prolonged if it arrives at the end of the predicted lifetime in good conditions.

Table 5.3 Time related power plant parameters.

Total plant lifetime	40 years
Blanket lifetime	22.72 years
Divertor lifetime	3.807 years
Availability fraction	0.75

6 Conclusions and future work

Nuclear fusion has the potentiality of becoming an important agent in the future energy market, but a long way must be walked before reaching this point. The ITER project must demonstrate the physical feasibility of obtaining net positive power before the construction of DEMO. In parallel, DEMO design must study all possible alternatives to ensure the best possible outcome. This work is framed in the balance of plant (BOP) of a future DEMO-like fusion reactor. A series of different S-CO_2 Brayton cycles have been proposed as the power cycle for reactors type DEMO1 (pulsed reactor, conservative design) and DEMO2 (steady-state reactor, optimistic design).

For DEMO1, the pulsed nature of the reactor has made mandatory the use of a thermal energy storage (TES) system. The nine studied layouts have modeled this TES through two approaches. With a simplified model that inputs the effect of the TES system directly at the electric efficiency and with a cycle model that changes depending on the source of the heat (from the reactor or from the storage system). Both models agree qualitatively in the results, but the TES model (the most accurate one) account for around 5% less efficiency. Layout A.1 has appeared as the most efficient one with a 34.4% efficiency, this layout features a recuperator at the compressor outlet, but it is constrained by the temperature limit set by the usage of water as coolant for divertor and shield. Two layouts were presented for a DEMO2-like reactor. In this case there were less restrictions and the efficiency got to 56%.

The economic analysis made with the PROCESS code has shown that a DEMO1-like power plant is not prepared to enter in the energy market if it is not heavily subsidized. DEMO2 could be market-ready as it presents a COE similar to thermal solar power, but it could still need public founding to keep the price low enough. Nonetheless, it is important to take into account that DEMO's goal is not bringing competitive prices to the energy market but to prove the technical feasibility of a fusion power plant and pave the way for a generation of commercial systems.

Next steps regarding DEMO1 include the study of the effect of different coolants for divertor and shield. Also, the TES model must be upgraded to take into account its inner consumption. For this, different TES technologies must be reviewed to found which one accommodates better to the idiosyncrasy of a fusion power plant. A turbomachinery model that changes the turbine and compressor efficiencies dynamically during the non-nominal

phase (when the cycle is being fed by the TES) is another intended upgrade for the code.

For DEMO2, a dedicated reactor model using the PROCESS code will be done, to change from the modified DEMO Baseline 2018 that was used for this work. This will improve the estimation of the electric power requirements of the reactor and ensure a more accurate electric plant efficiency and power production.

Bibliography

[1] Eurostat *Electricity production, consumption and market overview* *https://ec.europa.eu/eurostat/statistics-explained/index.php/Electricity_production,_consumption_and_market_overview#Electricity_generation*. Consulted November 2019

[2] European Environment Agency *Final energy consumption by mode of transport* *https://www.eea.europa.eu/data-and-maps/indicators/transport-final-energy-consumption-by-mode/assessment-9*. Consulted November 2019

[3] Nuclear Fusion *Plasma Physics and Fusion Energy* Public Domain, *https://commons.wikimedia.org/w/index.php?curid=1540082*. Consulted November 2019

[4] S. Gasstone & R. H. Lovberg *Controlled Thermonuclear Reactions* Robert E. Krieger Publishing Company, 1975

[5] C. P. João *Lasers, high power lasers and laser plasma interaction* Plasmasurf Summer School, Instituto de Plasmas e Fusão Nuclear Instituto Superior Técnico, Lisbon, Portugal, 2018

[6] Enciclopaedia Britannica *Ionization Energy* *https://www.britannica.com/science/ionization-energy*. Consulted November 2019

[7] V. Guerra *Introduction to plasma physics* Plasmasurf Summer School, Instituto de Plasmas e Fusão Nuclear Instituto Superior Técnico, Lisbon, Portugal, 2018

[8] M. Kikuchi & K. Lackner *Fusion Physics* International Atomic Energy Agency, 2012

[9] J. Freidberg *Plasma Physics and Fusion Energy* Cambridge University Press, 2007

[10] A. Dinklage *Basic plasma physics, fusion, the motion of charged particles in magnetic fields, magnetic confinement devices and aspects of safety* IPP Summer University, Max Planck Institute for Plasma Physics, Greifswald, Germany, 2018

[11] Nuclear Fusion *Stellarator* Public Domain, *https://commons.wikimedia.org/wiki/File:W7X-Spulen_Plasma_blau_gelb.jpg*. Consulted Novmeber 2019

[12] European Fusion Development Agreement *A roadmap to the realization of fusion energy* EFDA, 2012

[13] J.-M. Martinez *ITER vacuum vessel structural analysis completion during manufacturing phase* Fusion Engineering and Design, Number 109-111 S688-S692, 2016

[14] S. Konishi *DEMO plant design beyond ITER* Fusion Engineering and Design, Number 63-64 S11-S17, 2002

[15] S. Ishiyama *Study of steam, helium and supercritical CO_2 turbine power generations in prototype fusion power reactor* Progress in Nuclear Energy, Number 50 S325-S332, 2008

[16] H. Zhao *Optimized Helium-Brayton Power Conversion for Fusion Energy Systems* Fusion Science and Technology, Number 47:3 S460-S466, 2005

[17] J. Linares *Supercritical CO_2 Brayton power cycles for DEMO fusion reactor based on Helium Cooled Lithium Lead blanket* Applied Thermal Engineering, Number 76 S123-S133, 2015

[18] L. Vesely *Study of the cooling systems with S-CO_2 for the DEMO fusion power reactor* Fusion Engineering and Design, Number 124 S244-S247, 2017

[19] N. Taylor *Lesson learnt from ITER & licensing for DEMO and future nuclear fusion facilities* Fusion Engineering and Design, Number 89 S1995-S2000, 2014

[20] ITER *THE ITER TOKAMAK https://www.iter.org/mach*. Consulted November 2019

[21] M. Kovari *"PROCESS": A systems code for fusion power plants-Part 2: Engineering* Fusion Engineering and Design, Number 104 S9-S20

[22] S. Entler *Approximation of the economy of fusion energy* Energy, Number 152 S489-S497, 2018

[23] J. Linares *Technical report about steady-state and dynamic analysis* EFDA Technical Report, 2017

[24] D. Maisonnier *DEMO and fusion power plant conceptual studies in Europe* Fusion Engineering and Design, Number 81 S1123-S1130, 2006

[25] D. Maisonnier *The European power plant conceptual study* Fusion Engineering and Design, Number 75-79 S1173-S1179, 2005

[26] EFDA *A conceptual study for commercial fusion power plants - Final Report of the European Fusion Power Plant Conceptual Study (PPCS)* EFDA, 2005

[27] L.V. Boccaccini *Objectives and status of EUROfusion DEMO blanket studies* Fusion Engineering and Design, Number 109-111 S1199-S1206, 2016

[28] R. Wenninger *Advances in the physics basis for the European DEMO design* Nuclear Fusion, Number 55, 2015

[29] G. Federici *DEMO design activity in Europe: Progress and updates* Fusion Engineering and Design, Number 136 S729-S741, 2018

[30] Wikipedia *Tritium* https://en.wikipedia.org/wiki/Tritium. Consulted December 2019

[31] M. Kovari *"PROCESS": A systems code for fusion power plants-Part 1: Physics* Fusion Engineering and Design, Number 89 S3054-S3069

[32] M. J. D. Powell *A Hybrid Method for Non-linear Algebraic Equations* Numerical Methods for Non-linear Algebraic Equations ed. P. Rabinowitz, Prentice-Hall

[33] R. L. Crane *Solution of the General Nonlinear Programming Problem with Subroutine VMCON* Argonne National Laboratory Report ANL-80-64, 1980

[34] P. J. Knight *A User Guide to the PROCESS Fusion Reactor Systems Code* Culham Centre for Fusion Energy, 2016

[35] C. Ortiz *Power cycles integration in concentrated solar power plants with energy storage based on calcium looping* Energy Conversion and Management, Number 149 S815-S829, 2017

[36] R. Chacartegui *Alternative cycles based on carbon dioxide for central receiver solar power plants* Applied Thermal Engineering, Number 31 S872-S879, 2011

[37] Wikipedia *Brayton Cycle* https://es.wikipedia.org/wiki/Archivo:Brayton_cycle.svg. Consulted March 2020

[38] J. Linares *Design, modelling and analysis of primary heat transfer and BoP options for integration with a DEMO fusion power plant: State of the Art in supercritical CO_2 Brayton power cycles.* EUROfusion, 2013

[39] Sulzer Bros *Sulzer Patent Verfhren zur Erzeugung von Arbeit aus Warme* Swiss Patent 269 599, 1948

[40] E. G. Feher *The Supercritical Thermodynamic Power Cycle* Energy Conversion, Number 8 S85-S90, 1968

[41] G. Angelino *Carbon Dioxide Condensation Cycles for Power Production* ASME Paper No. 68-GT-23, 1968

[42] D. P. Gokhstein *Use of Carbon Dioxide as a Heat Carrier and Working Substance in Atomic Power Station* Soviet Tomic Energy, 26, 1969

[43] J. R. Hofman *150 kWe Supercritical Closed Cycle System* ASME paper no. 70-GT-89, 1970

[44] V. Dostal *A Supercritical Carbon Dioxide Cycle for Next Generation Nuclear Reactors* MIT, 2004

[45] R. Chacartegui *Thermochemical energy storage of concentrated solar power by integration of the calcium looping process and a CO_2 power cycle* Applied Energy, Number 173 S589-S605, 2016

[46] O. V. Combs *An Investigation of the Supercritical CO_2 Cycle (Feher Cycle) for Shipboard Application* MIT, 1977

[47] S. Mirofci *A supercritical fluid extraction process to obtain valuable compounds from Eruca Sativa leaves* Università degli Studi di Padova, 2014

[48] S. A. Wright *Thermo-Economic Analysis of Four sCO_2 Waste Heat Revoery Power Systems* SCO2 Symposium, 2016

[49] F. Crespi *Supercritical carbon dioxide cycles for power generation: A review*

[50] EES *EES* http://fchartsoftware.com/ees/. Consulted February 2020

[51] R. Span *A New Equation of State for Carbon Dioxide Covering the Fluid Region from the Triple-Point Temperature to 1100 K at Pressures up to 800 MPa* Journal of Physical and Chemical Reference Data, Number 25, 1996

[52] E. Cipollini *Alternative range of viable secondary coolants and options for thermodynamic cycles* EUROfusion, 2014

[53] J. Linares *Technical Report about steady-state and dynamic analysis* EUROfusion, 2017

[54] J. Linares *Sizing of a recuperative supercritical CO2 Brayton cycle as power conversion system for DEMO fusion reactor based on Dual Coolant Lithium Lead blanket* Fusion Engineering and Design, Number 134 S79-S91, 2018

[55] D. Sanchez *Performance analysis of a MCFC and supercritical carbon dioxide hybrid cycle under part load operation* International Journal of Hydrogen Energy, Number 36 S10327-S10336, 2011

[56] Z. Ma *Thermal Energy Storage and Its Potential Applications in Solar Thermal Power Plants and Electricity Storage* ASME 2011 5th International Conference of Energy Sustainability, 2011

[57] Grupo de Máquinas y Motores Térmicos, US *Lección 13. Ciclos regenerativo y compuesto de la turbina de gas.* Máquinas y Motores Térmicos, 2017

[58] IRENA *REthinking Energy 2017* *https://www.irena.org/DocumentDownloads/Publications/IRENA_REthinking_Energy_2017.pdf*. Consulted April 2020

[59] L. Argote *Learning Curves in Manufacturing* Science, Number 4945 S920-S924, 1990

[60] S. Novak *Nuclear power plant ageing and life extension: Safety aspects* IAEA Bulletin, 1987